



Laporan Akhir Projek Penyelidikan Jangka Pendek

**Formation of Nanotubular TiO₂ Bioactive
Oxide Layer on Titanium and Cell
Response Studies**

by

Assoc. Prof. Dr. Srimala Sreekantan

Prof. Zainal Arifin Ahmad

Mr. Ishak Mat

Norehan Mokhtar

2011



FINAL REPORT
FUNDAMENTAL RESEARCH GRANT SCHEME (FRGS)
Laporan Akhir Skim Geran Penyelidikan Asas (FRGS) IPT
Pindaan 1/2010

A RESEARCH TITLE : Formation of Nanotubular TiO₂ Bioactive oxide layer on titanium and cell response
Tajuk Penyelidikan

PROJECT LEADER : Srimala Sreekantan *Im D1*
Ketua Projek

PROJECT MEMBERS : 1. Zainal Arifin Ahmad *Dwi*
 (including GRA) 2. Ishak Mat
 3. Norehan Mokhtar
Ahli Projek

PROJECT ACHIEVEMENT (Prestasi Projek)

B

ACHIEVEMENT PERCENTAGE					
Project progress according to milestones achieved up to this period	0 - 50%		51 - 75%		76 - 100%
Percentage (based on the revised objectives and milestone)					X
RESEARCH OUTPUT					
Number of articles/ manuscripts/ books (Please attach the First Page of Publication)	Indexed Journal		Non-Indexed Journal		
	1 (Journal of Nanomaterials) <i>Prove Attached in Appendix A</i>		0		
Conference Proceeding (Please attach the First Page of Publication)	International		National		
	0		0		
Intellectual Property (Please specify)					
HUMAN CAPITAL DEVELOPMENT					
Human Capital	Number				Others (please specify)
	On-going		Graduated		
Citizen	Malaysian	Non Malaysian	Malaysian	Non Malaysian	
PhD Student					
Master Student					
Undergraduate Student			2		
Total			2		

EXPENDITURE (Perbelanjaan)

C Budget Approved (Peruntukan diluluskan) : RM 24,000.00
 Amount Spent (Jumlah Perbelanjaan) : RM 31,766.53
 Balance (Baki) : RM -7,766.53
 Percentage of Amount Spent : 132.00 %
 (Peratusan Belanja)

Account Statement is attached in Appendix B

ADDITIONAL RESEARCH ACTIVITIES THAT CONTRIBUTE TOWARDS DEVELOPING SOFT AND HARD SKILLS
 (Aktiviti Penyelidikan Sampingan yang menyumbang kepada pembangunan kemahiran insaniah)

D

International		
Activity	Date (Month, Year)	Organizer
(e.g : Course/ Seminar/ Symposium/ Conference/ Workshop/ Site Visit)	0	
National		
Activity	Date (Month, Year)	Organizer
(e.g : Course/ Seminar/ Symposium/ Conference/ Workshop/ Site Visit)	0	

PROBLEMS / CONSTRAINTS IF ANY (Masalah/ Kekangan sekiranya ada)

E We only manage to complete a portion of the proposed project for the budget approved for this work not sufficient to complete all the objectives. The cell interaction is not investigated in detail for the budget approved only 24, 000 and it is certainly not sufficient for such studies. Therefore we just manage to work on the formation of TiO₂ nanotubes on Ti alloys which supplied by Straits Orthopaedics.

RECOMMENDATION (Cadangan Penambahbaikan)

F Hope the budget allocated is adequate to conduct comprehensive work on such studies. This will allow us to understand the fundamental knowledge lies in the project an propose mechanistic model of such cell interaction on nanotubular structure. This ultimate output will contribute to the field of health science.

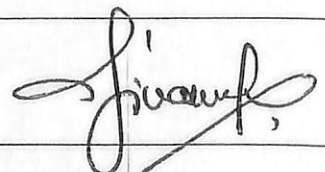
RESEARCH ABSTRACT – Not More Than 200 Words (*Abstrak Penyelidikan – Tidak Melebihi 200 patah perkataan*)

G This work focus on the formation of titanium oxide (TiO₂) nanotubes on the Ti-6Al-4V alloy by anodization method in organic ethylene glycol electrolyte (EG). The dimension of nanotubes could be tuned by changing the electrochemical parameters such as NH₄F content, voltage applied; and anodization time. The average nanoporous or nonotube diameter and length were found to increase with increasing amount of fluoride, anodization voltage and anodization time. Minimum of 0.5 g NH₄F is required for growth of nanotubes. TiO₂ nanotubes with average diameter of 110 nm and 3.1 μm lengths were obtained in EG containing 0.7 g NH₄F. Upon annealing from temperature 400°C to 600°C in argon atmosphere shows crystallization of the nanotubes to anatase phase exists at 400°C while rutile dominantly exists at 600°C. Anodization in the organic electrolyte resulted in homogeneous structure unlike the one reported in aqueous acidified fluoride solution which resulted in inhomogeneous structure due to the severe attack of the β-phase. For the case of behavior of cell interaction using human foreskin fibroblast cells line (HS27) studies shown that amorphous TiO₂ nanotubes structure has better cellular interaction as compare to anatase and rutile crystal structure.

The Full technical report is attached in Appendix C

Date : 24 Aug 2011
Tarikh

Project Leader's Signature:
Tandatangan Ketua Projek



COMMENTS, IF ANY/ ENDORSEMENT BY RESEARCH MANAGEMENT CENTER (RMC)

(Komen, sekiranya ada/ Pengesahan oleh Pusat Pengurusan Penyelidikan)

H

Projek ni sudah melampaui pelayan pasca-siswazah.
Badei projek negatif.

Name:
Nama:

Signature: :
Tandatangan:



Date:
Tarikh:

21/7/12

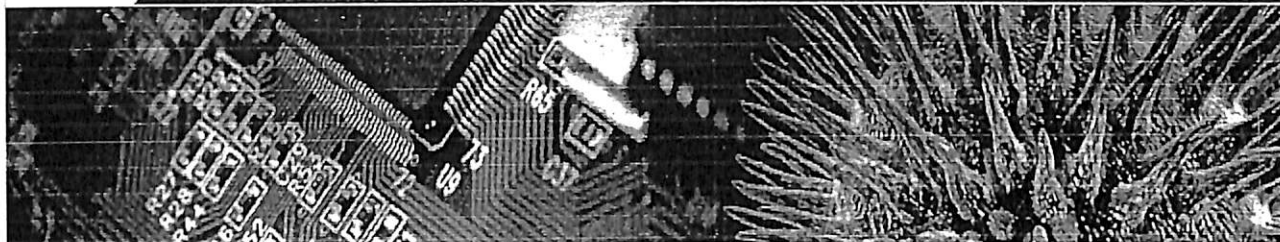
Appendix A

Publication



Hindawi

Ramarao Poliah [Update My Account](#) [Logout](#)



Author Activities

239289.v3 (Research Article)

Title	Characterization and photocatalytic activity of enhanced copper-silica loaded titania prepared via hydrothermal method
Journal	Journal of Nanomaterials
Issue	Regular
Additional Files	Reply to review reports
Manuscript Number	239289.v3 (Research Article)
Resubmitted On	2011-06-23
Authors	Ramarao Poliah, Srimala Sreekanta
Editor	Edward Andrew Payzant (Assigned on 2011-06-23)
Editorial Recommendation	Publish Unaltered (Made On 2011-07-13)
Editorial Decision	Accepted (Made On 2011-07-13)

Characterization and photocatalytic activity of enhanced copper-silica loaded titania prepared via hydrothermal method

Ramarao Poliah¹, Srimala Sreekantan^{1*}

¹*School of Materials and Mineral Resources Engineering, Universiti Sains Malaysia, Engineering Campus, Nibong Tebal, Seberang Perai Selatan, Pulau Pinang 14300, Malaysia.
Email: ramarao2609@gmail.com, srimalala@eng.usm.my*

**Corresponding author.*

School of Materials and Mineral Resources Engineering, Universiti Sains Malaysia, Engineering Campus, Nibong Tebal, Seberang Perai Selatan, Pulau Pinang 14300, Malaysia.

Tel: +60 4 5995255; Fax: +60 4 5941011

E-mail: srimalala@eng.usm.my (S. Sreekantan).

Abstract

TiO₂ nanopowder, loaded with SiO₂ and Cu-SiO₂, was prepared under both acidic and basic environments via the hydrothermal method. The morphology and structure of TiO₂ were studied by XRD, TEM and FT-IR. The photocatalytic activity of samples was studied by monitoring the degradation of methyl orange, using a UV-visible spectrophotometer. The effect of Ti/Si ratio, pH, and Cu²⁺ addition on the formation of TiO₂ and its photocatalytic activity were investigated in detail. The results show that a large surface area and a high surface acidity were important factors to achieve good TiO₂ performance. The presence of Ti-O-Si bonding enhanced surface acidity, which improved its ability to adsorb more hydroxyl radicals and increased its surface area. Addition of 0.1mol% concentration of Cu²⁺ and 25mol% SiO₂ in TiO₂ induced the formation of new states close to the conduction band, which narrowed the band gap energy and enhanced the photodegradation efficiency.

Keywords: Titania; Silica; Copper; Hydrothermal; Photocatalytic activity; pH

1.0 Introduction

In recent years, cases of air and water pollution have been increasing due to the continuous rise in population and urbanization. Improper waste management has been identified as one of the prime factors that contribute to the pollution. In 2003, the average amount of municipal solid waste (MSW) generated in Malaysia was 0.5–0.8 kg/person/day, which has further increased to 1.7 kg/person/day in major cities [1]. Solid waste management continues to be a major challenge throughout the world, particularly in rapidly growing cities and towns [2].

Land filling and incineration are two of the most common methods of solid waste disposal. Unlike land filling, incineration requires minimum land, reduces the volume of solid waste by half, and can be operated in any weather. Nevertheless, emission of pollutants, especially dioxin and furan, is the major drawback of incineration. Among the various solutions available, photocatalysis is considered to be a green technique that has great potential to decompose contaminants without leaving harmful intermediates [3–5]. Choi et al. reported that the polychlorinated dibenzo-p-dioxins such as mono-, tetra-, hepta-, and octachlorinated congeners were successfully degraded by a TiO₂ film under UV or solar light irradiation [6].

Titanium dioxide is the most promising photocatalyst due to its superior properties such as low cost, environmental compatibility, and long term photochemical stability [7–10]. However, its wide band gap energy (3.0 for rutile; 3.2 for anatase) limits its use as a photocatalyst in various applications. The large surface area, high crystallinity, low crystallite size, and crystal structure are important properties that influence the photocatalytic activity of TiO₂. In recent years, much effort has been directed toward TiO₂ modification to enhance its photocatalytic activity [11–15]. For instance, TiO₂ loaded with various secondary oxides such as ZrO₂ [16], WO₃, MnO₂, CuO, V₂O₅, Al₂O₃ [17] and transition metals salt such as Cu²⁺ [18] and Fe²⁺ [19,20], has been reported to be a more efficient photocatalyst than pure TiO₂. The composite TiO₂-SiO₂ has attracted great interest because of its ability to prevent the grain

growth of TiO₂ particles and enhance the thermal stability for the phase transformation of TiO₂ from anatase to rutile [21–27]. Xu et al. [24] studied the effect of a wide range of SiO₂ levels added to the microstructure and the photocatalytic activity of TiO₂ powder; preparation involved the sol-gel method and calcination at various temperatures. Addition of SiO₂ resulted in a marked reduction in grain size and an increase in the surface area of the catalyst. Results of other studies are summarized in Table 1. Although many reports describe the effect of SiO₂ on the photocatalytic activity of TiO₂, the results do not agree with one another, possibly due to differences in the processing methods or experimental conditions. On the other hand, Chen et al. [18] has been reported that 0.1wt% of Cu²⁺ doped TiO₂-SiO₂ showed higher photocatalytic activity than that of undoped TiO₂-SiO₂. The effects of pH value on pure TiO₂ formation have been reported by several groups [28,29]. Yu et al. prepared TiO₂ powder at different pH values through the hydrothermal method [28]. They found that the pH value of the starting solution has a significant effect on the crystallinity, crystallite size, phase structure, and photocatalytic activity of the synthesized TiO₂ powder. They proposed that basic conditions are favorable for the formation of pure anatase. Samples prepared at pH 9 display higher photocatalytic activity. However, this result contradicts those obtained by Karami et al. [29], who concluded that TiO₂ prepared under acidic conditions (pH 3) through the sol-gel method has higher photocatalytic activity.

Although the sol-gel method is widely used due to its simplicity and low cost, calcination in air is required for the formation of the anatase phase from amorphous TiO₂. Li et al. [26] did a comparative study of the sol-gel and hydrothermal methods for the synthesis of TiO₂-SiO₂ composite nanoparticles, and found that samples prepared through the hydrothermal route still possess a stable anatase phase, a large specific surface area, a small particle size, and a high photocatalytic activity, even when calcined at 1000 °C. However, they did not report the effect of pH on the formation of TiO₂-SiO₂ nanoparticles. In the present study, the effect of pH values on photocatalytic activity and the optimum Ti/Si ratio for photocatalytic activity of TiO₂

powder prepared by hydrothermal method were examined. The effect of Cu-SiO₂ addition on

the phase structure and the photocatalytic activity of TiO₂ were also studied.

2.0 Experimental Procedure

2.1 Preparation

Initially, the oxide powder TiO₂-SiO₂ with various Ti/Si ratios at pH 3 and 9 were prepared, and the photocatalytic performance was evaluated to select the optimum Ti/Si ratio.

The Ti/Si ratios and pH values in the experiment are summarized in Table 2. Tetraethylorthotitanate (TEOS) with a normal purity of 97% (Aldrich, US) and tetraethylorthosilicate (TEOS) with a normal purity of 98% (Merck, Germany) were used as the source of titanium and silicon, respectively. Both were dissolved in equal volumes of ethanol,

after which a few drops of hydrochloric acid were added to TEOS as catalyst. Afterward, the mixture was kept in a water bath maintained at 70 °C for 2 h. The TEOS and TBOT precursors were then mixed and stirred for 15 minutes before adding the desired amount of copper(II) nitrate. The pH values were adjusted by adding hydrochloric acid for the acidic condition, and sodium hydroxide for the basic condition. This solution was stirred for 1 h at room temperature

and then cooled to room temperature. The sample obtained was washed and then dried at 100 °C. A powder was obtained.

2.2 Characterization and photocatalytic degradation

The powder samples were characterized by X-ray diffraction (XRD) using a Bruker D8 powder diffractometer employing Cu K α radiation. The accelerating voltage and the applied current were 40 kV and 40 mA, respectively. The average crystallite size of the TiO₂-SiO₂ oxide powder was calculated using X-ray line broadening methods based on the Scherrer formula. Additionally, the morphology of the powder was observed by transmission electron microscopy (TEM) using a Philips 420T. The chemical structure information of the particles

Table 1 Photocatalytic activity of TiO₂ with various SiO₂ content

Ti/Si Ratio (%)	Preparation Method	Crystallite Size (nm)	Phase Structure	Photocatalytic Activity (%)
1:1 (50%) [18]	Sol-gel (100 °C, 1 h)	5-8	A: 100%	90 (MB, 2 h)
1:1 (50%) [19]	Sol-gel (100 °C, 9 h)	100-120	A: 100%	95 (Rhodamine B, 2 h)
19:1 (5%) [20]	Sol-gel (500 °C, 1 h)	6.7	A: 100%	73 (MO, 1 h)
3:1 (25%) [21]	Sol-gel (550 °C, 2 h)	4.5 (A) 9.2 (R)	A: 43.3%	65 (MO, 2 h)
7:3 (30%) [22]	Sol-gel (800 °C, 2 h)	12	A: 100%	92 (MO, 5 h)
3:2 (40%) [23]	Hydrothermal (140 °C, 10 h)	7	A: 100%	95 (MB, 1 h)
3:1 (25%) [24]	Hydrothermal (200 °C, 24 h)	16.3	A: 100%	80 (MB, 8 h)

A = anatase, R = rutile, MB = methyl blue, MO = methyl orange

was obtained by Fourier transform infrared spectroscopy (Spectrum One, Perkin Elmer, US). Photocatalytic degradation studies were performed using 30 mg/L methyl orange (MO) solution. A total of 0.1 g TiO₂-SiO₂ oxide powder was added to 30 mL of MO solution and photoirradiated for 1 h at room temperature using a TUV 18W UV-C Germicidal light. The concentration of the degraded MO was determined using a UV-visible spectrophotometer (Varian, Cary 50 Conc).

Table 2 Crystal properties of TiO₂-SiO₂ oxide powder

Sample	Ti/Si Ratio	SiO ₂ Content (%)	Final pH value	Crystallite size/nm (XRD)
SA0	1 : 0	0	3	6.30
SA 5	19 : 1	5	3	6.63
SA10	9 : 1	10	3	7.06
SA16	5 : 1	16.67	3	8.91
SA20	4 : 1	20	3	9.54
SA25	3 : 1	25	3	6.88
SA25-Cu(0.05)	3 : 1	25	3	10.8
SA25-Cu(0.1)	3 : 1	25	3	9.48
SA25-Cu(0.15)	3 : 1	25	3	9.62
SA25-Cu(0.2)	3 : 1	25	3	10.11
SA25-Cu(0.5)	3 : 1	25	3	8.21
SA25-5	3 : 1	25	5	8.63
SN25-7	3 : 1	25	7	9.98
SA30	7 : 3	30	3	11.78
SA50	1 : 1	50	3	11.76
SB0	1 : 0	0	9	3.75
SB16	5 : 1	16.67	9	-
SB20	4 : 1	20	9	-
SB25	3 : 1	25	9	-
SB25 - 12	3 : 1	25	12	-
SB25 - 14	3 : 1	25	14	4.57
SB30	7 : 3	30	9	-
SB50	1 : 1	50	9	-

SA = Acid, SB = Basic, SN = Neutral

3.0 Results and discussion

3.1 Effect of SiO₂ content

XRD was used to analyze the formation of the crystalline phase of the TiO₂ powder prepared with various amounts of SiO₂ in both acidic and basic environments. Figure 1 illustrates the XRD patterns of TiO₂ prepared at pH 3 with various Ti/Si ratios. The TiO₂ prepared at various Ti/Si ratios led to formation of the anatase phase. Patterns of samples without SiO₂ (SA0) shows peak for anatase and a small peak for the brookite phase at a diffraction angle of ~20°. The relative intensities of the anatase diffraction peaks in each sample are different; this suggests that the degree of crystallinity is affected by the SiO₂ content. A high crystallinity of TiO₂ was obtained with addition of 30 mol% SiO₂ (SA30), whereas low crystallinity was observed in samples with 25 mol% SiO₂ (SA25). No SiO₂ crystal phase was identified in all samples. This indicates that SiO₂ existed as an amorphous phase in the TiO₂-SiO₂ composite.

The formation of brookite phase in sample SA0 (acidic condition) could be explained as follows [28]: Ti(OH)_x(OC₄H₉)_{4-x} forms as a result of hydrolysis reaction between TBOT and HCl where x was related to the pH value of starting solution. Since the ligand field strength of Cl⁻ ions was larger than that of butoxy group in HCl solution, thus the Cl⁻ ions could substitute the butoxy group in the Ti(OH)_x(OC₄H₉)_{4-x} complex and led to the formation of complex Ti(OH)₂Cl₂. The complex Ti(OH)₂Cl₂ actually existed in the form of Ti(OH)₂Cl₂(H₂O)₂ in a solution due to the Ti(IV)(3d⁰) complex ions are all octahedrally coordinated in solution and crystal. It is reported that Ti(OH)₂Cl₂(H₂O)₂ could be the precursor of brookite. This mechanism was favored to explain the occurrence of brookite in the sample.

The XRD patterns of TiO₂ prepared at pH 9 with various Ti/Si ratios (not shown here) shows samples prepared without SiO₂ (SB0) produced peaks characteristic of anatase at 2θ of 24, 34, 39, and 48°, and the peak of rutile at 28°. However, the peak intensity of this sample is

very low compared to those produced by samples prepared under acidic conditions; this indicates that the phase transformation to anatase or rutile was not fully achieved at basic conditions. In contrast, samples prepared with SiO₂ generally showed amorphous TiO₂. In basic conditions, Na⁺ attacks the Ti-O-Ti bond, which results in the formation of a two-dimensional layered structure with dangling bonds that contribute to the formation of the amorphous phase. This is in good agreement with the TEM analysis which is discussed later.

The crystallite size of the TiO₂-SiO₂ powders prepared in acidic condition was calculated using Scherrer formula, and plotted against SiO₂ content. Figure 2 shows a non-linear relationship between the crystallite size and the amount of added SiO₂. The trend is contrary to results in the literature wherein SiO₂ addition was found to retard grain growth of TiO₂ and therefore reduce its crystallite size [23,24,26]. In the present study, the lowest crystallite size was 6.3 nm for pure TiO₂ (SA0), and increased gradually with further addition of SiO₂. However, the crystallite size of TiO₂ for sample SA25 decreased drastically as the SiO₂ amount reached 25 mol%; this may be attributed to the large surface area of the sample. Binary metal oxides are known to induce surface acidity [30]. The FTIR spectra of the TiO₂-SiO₂ powder at various SiO₂ contents are shown in Figure 3. When the SiO₂ content reached 25 mol%, a small peak at 960 cm⁻¹ corresponding to the Ti-O-Si bond was observed. The presence of this oxide might have increased the surface acidity of the sample. Higher surface acidity led to a higher degree of adsorption of the OH radicals (1640 cm⁻¹) and resulted in a larger surface area. The surface area was inversely proportional to grain size. The Ti-O-Si band intensity increased with addition of 30–50 mol% SiO₂, and the intensity of bands for the hydroxyl group decreased. These indicate that large amounts of SiO₂ (30–50 mol%) in TiO₂ cannot effectively improve the surface acidity and prevent the growth of TiO₂ grains. Therefore, in sample SA25, SiO₂ effectively enhanced the surface acidity, suppressed the grain growth of TiO₂, and produced smaller crystallite size. The peak for the asymmetric stretching of Si-O-Si at 1060 cm⁻¹ clearly increased with addition of SiO₂, whereas the band intensity at 400–700 cm⁻¹ (vibration of Ti-O

bonds in Ti-O-Ti bonding) decreased. Therefore, the intensity of the peak for the Si-O-Si bond was inversely proportional to the intensity of the peak for the Ti-O-Ti bond.

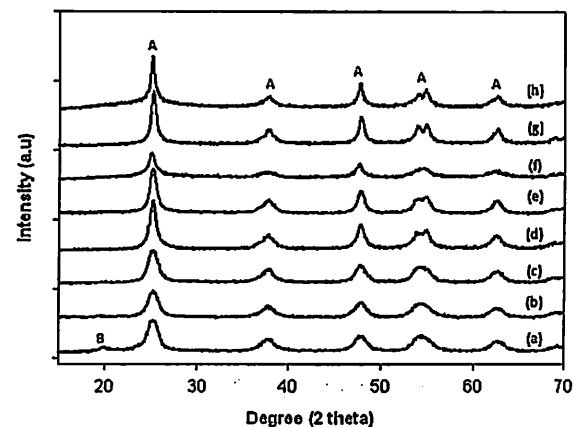


Figure 1 XRD patterns of the TiO₂ powder prepared with different amounts of SiO₂ at pH 3: (a) 0 mol%, (b) 5 mol%, (c) 10 mol%, (d) 16 mol%, (e) 20 mol%, (f) 25 mol%, (g) 30 mol%, (h) 50 mol%. (A: anatase, B: brookite)

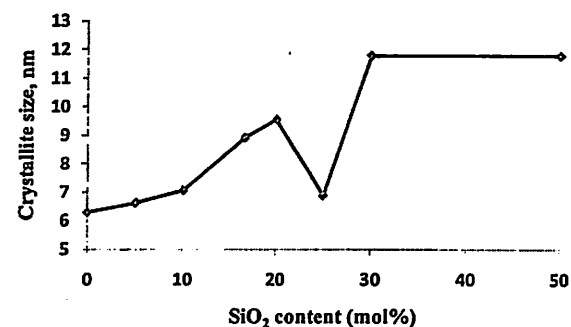


Figure 2 Relationship between the crystallite size and amount of SiO₂ on TiO₂ powder prepared at pH 3.

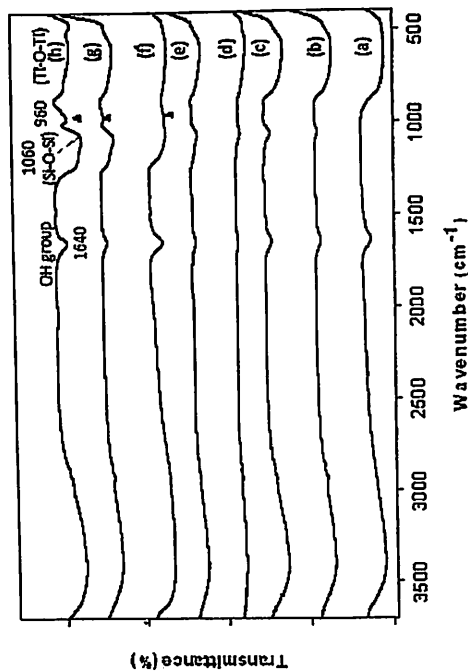


Figure 3 FTIR spectra of $\text{TiO}_2\text{-SiO}_2$ oxide powder containing SiO_2 : (a) 0 mol%, (b) 5 mol%, (c) 10 mol%, (d) 16 mol%, (e) 20 mol%, (f) 25 mol%, (g) 30 mol%, (h) 50 mol%. ▲ indicates absorption bands at 960 cm^{-1} , which is characteristic of Ti-O-Si bonding.

3.2 Effect of pH value

Figure 4 shows the XRD pattern of TiO_2 powder with 25mol% SiO_2 ($\text{TiO}_2\text{-25mol}\%$ SiO_2) at various levels of pH. In the presence of SiO_2 , an acidic condition was favorable to form anatase structure. As the system is shifted from acidic to neutral, the intensity of the anatase peak ($2\theta = 25^\circ$) and the crystallite size increased. Thus, pH value also affected the degree of crystallinity despite the presence of SiO_2 . At pH 12, the crystal structure of sample SB25-12 could not correspond to anatase, rutile or brookite. It was similar to that of $\text{Na}_2\text{O}_7\text{Ti}_3$ [31], $\text{H}_2\text{O}_2\text{Si}_2\text{Ti}_4$ and $\text{H}_4\text{Na}_4\text{O}_{16}\text{Si}_4\text{Ti}_2$ probably due to their same layered titanate family [32]. Further increase in basic condition (pH 14) resulted in formation of the partial anatase phase, as seen in the TEM images of $\text{TiO}_2\text{-25mol}\%$ SiO_2 powders prepared at various pH values in Figure 5. Spherical like particles (Figure 5a and b) were observed in samples prepared in acidic and

neutral conditions. At pH 12, a lamellar structure (two-dimensional layered structures) formed as a result of the reaction between the sample and NaOH (Figure 5c), which involved attack of Na^+ on the Ti-O-Ti bond. The edges of the lamellar structure might have many atoms with dangling bonds with enough energy to destabilize the two-dimensional structures [33]. As the system shifted toward high pH, the lamellar TiO_2 deformed to saturate the dangling bonds. At pH 14, the transition three- → two- → one dimension was almost complete, while the lamellar structure formed tubes (Figure 5d); this resulted in a partial anatase phase. Thus, the pH appeared to have a significant effect on TiO_2 phase structure and morphology.

Figure 6 illustrates the FTIR transmission spectra of $\text{TiO}_2\text{-25 mol}\%$ SiO_2 powder prepared at various pH values and autoclaved at 150°C for 24 h. The spectrum of pure TiO_2 is also included as reference. The broad peaks at 3400 cm^{-1} and the peaks at 1640 cm^{-1} in all spectra are attributed to surface-adsorbed water and the bending mode of hydroxyl groups. The surface-adsorbed water and hydroxyl group decreased slightly as the pH increased; this is possibly due to the reduction in surface area of the sample, which prevented further water vapor absorption. This is consistent with the results wherein samples prepared at pH 3 had higher photocatalytic activity compared with those prepared at pH 7. The peaks, which were absent in pure TiO_2 , appeared at 960 cm^{-1} and $1040\text{-}1070\text{ cm}^{-1}$ due to the Ti-O-Si stretching and the asymmetric stretching vibration of Si-O-Si, respectively. These peaks gradually decreased and eventually disappeared at higher pH. This implies that the Ti-O-Si bonds weakened as the pH increased. The stretching vibration of Ti-O bonds in Ti-O-Ti can be observed at $400\text{-}700\text{ cm}^{-1}$. Peaks related to carboxyl groups were observed at the $1340\text{-}1470\text{ cm}^{-1}$ range. The carboxyl groups might be a result of oxidation of organic species during hydrothermal treatment [28]. As the preparation conditions shifted from acidic to basic, the oxidation process was inhibited; this caused the peaks to disappear completely.

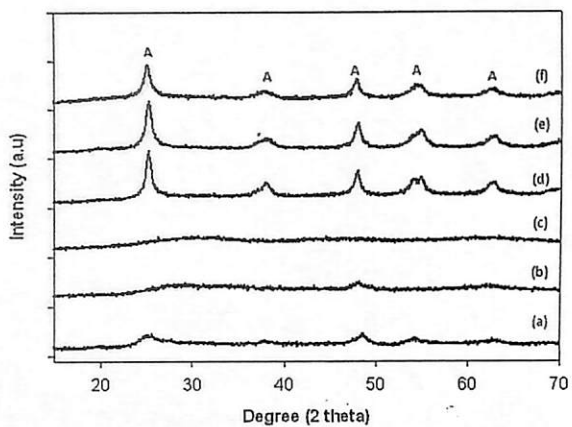


Figure 4 XRD pattern of 25 mol% SiO₂-loaded TiO₂ powder at various pH values: (a) pH 14, (b) pH 12, (c) pH 9, (d) pH 7, (e) pH 5, (f) pH 3. (A: anatase)

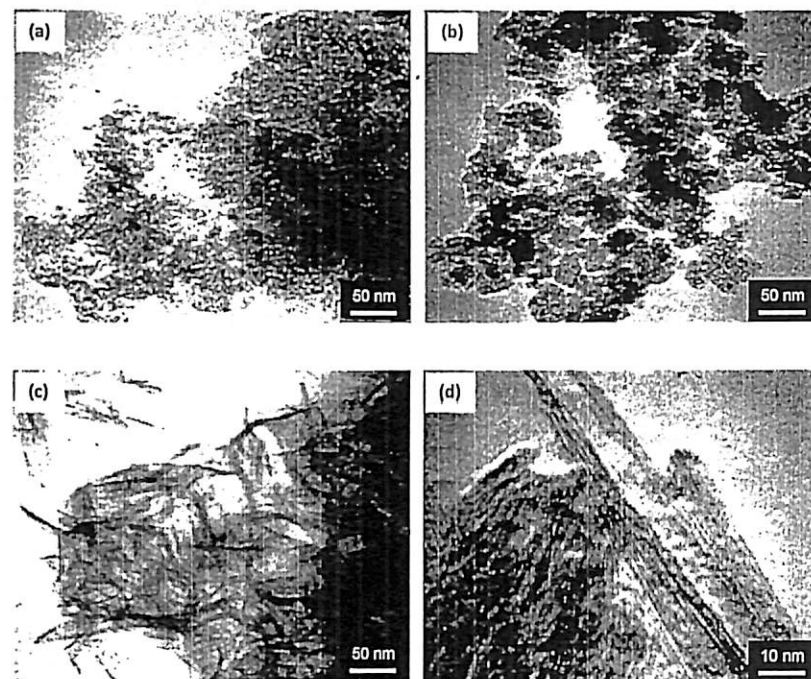


Figure 5 TEM images of TiO₂-25% SiO₂ oxide powder prepared at various pH values: (a) pH 3, (b) pH 7, (c) pH 12, (d) pH 14.

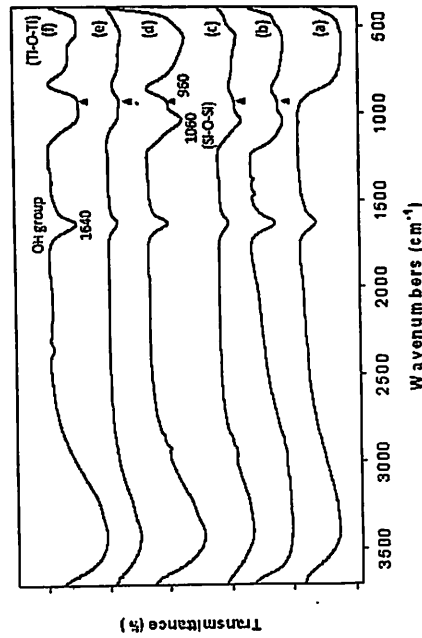


Figure 6 FTIR spectra of TiO_2 -25% SiO_2 oxide powder prepared at various pH values: (a) pure TiO_2 (pH 3), (b) pH 3, (c) pH 5, (d) pH 7, (e) pH 9, (f) pH 12.

▲ indicates absorption bands at 960 cm^{-1} , which is characteristic of Ti-O-Si bonding.

3.3 Effect of Cu^{2+} addition in TiO_2 - SiO_2 powder

The XRD patterns of Cu^{2+} -loaded TiO_2 - SiO_2 are shown in Figure 7. The TiO_2 - SiO_2 loaded with various amounts of Cu^{2+} , maintained an anatase phase. The presence of Cu^{2+} was hardly detected by XRD due to its low content. However, the relative intensities of the anatase peak vary among samples. High TiO_2 crystallinity was obtained with addition of 0.2 mol% Cu^{2+} and lower degrees of crystallinity were observed in samples containing 0.5 mol% copper, which were due to the poor distribution of Cu^{2+} in the TiO_2 matrix. The TiO_2 without Cu^{2+} produced relatively small diffraction peaks of anatase at 25° (101), in contrast to the patterns of the samples with Cu^{2+} . Therefore, phase transformation was not fully achieved without Cu^{2+} , as the TiO_2 retained portions of the inactive amorphous phase.

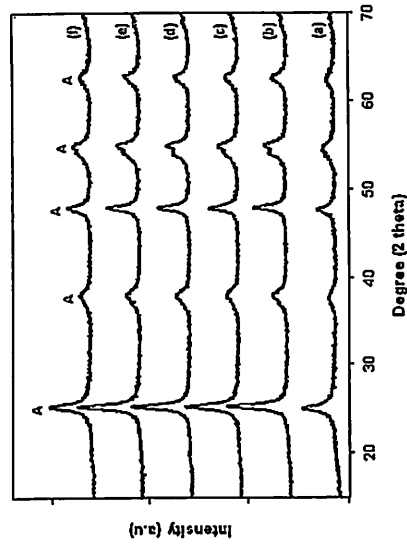


Figure 7 XRD pattern of 25% SiO_2 -loaded TiO_2 powder with various copper contents: (a) 0 mol%, (b) 0.05 mol%, (c) 0.1 mol%, (d) 0.15 mol%, (e) 0.2 mol%, (f) 0.5 mol%.

(A: anatase)

3.4 Photocatalytic activity

The photocatalytic activity of the TiO_2 - SiO_2 powder, prepared under acidic and basic conditions was evaluated through the degradation of methyl orange (MO) under ultraviolet light irradiation for 1 h at room temperature. Evaluation was repeated for 3 times and average values were plotted. Samples prepared in acidic conditions displayed photocatalytic activity higher than that of samples prepared in basic conditions (Figure 8). This is attributed to the presence of anatase in the samples prepared under acidic conditions. Photocatalytic activities of the samples with different Ti/Si ratio vary. Pure TiO_2 (SAO) prepared in acidic conditions resulted in high photocatalytic activity. However, addition of 2.5 and 50 mol% of SiO_2 in TiO_2 produced the highest photocatalytic activity compared with pure TiO_2 . Thus, the presence of SiO_2 was essential to higher photocatalytic activity. As the SiO_2 present in TiO_2 promoted a high degree of anatase crystallinity, a lower crystallite size was produced due to suppression of TiO_2 grain

growth. This might have contributed to the larger surface area of the TiO_2 particles. The addition of SiO_2 in TiO_2 also enhanced the acidity of the binary oxide. A model has been proposed to explain this increase in acidity [34]. In this model, the silicon cation enters the lattice of the host oxide, TiO_2 , and retains its original coordination number. Since the silicon cation is still bonded to same number of oxygen atoms despite coordination changes in the oxygen atoms, a charge imbalance is created. The charge imbalance must be satisfied. Thus, Lewis sites are expected to form due to the positive charge in the $\text{TiO}_2\text{-SiO}_2$. The surface with improved acidity can adsorb more OH radicals, thus resulted in a larger surface area. This might enhanced the photocatalytic activity and led to complete degradation of MO. This is consistent with the FTIR results of the sample (pH 3) possessed high intensity of hydroxyl group. The result also indicates that samples prepared at basic conditions showed the poor MO degradation, which is in agreement with the observations of Yu et al. [23]. They revealed that amorphous TiO_2 has a lower photocatalytic activity compared with crystalline TiO_2 . Hence, SiO_2 -loaded TiO_2 powder prepared under basic conditions is inefficient for high photodegradation.

To understand the degradation of MO with time, samples were irradiated and collected every 15 min. Pure TiO_2 showed rapid degradation at the beginning, which eventually remained constant after 15 min (Figure 9). This is due to the low anatase concentration of TiO_2 , and its inherent structure and low surface area. The TiO_2 with 25 and 50 mol% SiO_2 had low degradation rate during the first 15 min. Afterward, degradation markedly increased; both samples completely degraded MO within 1 h. It is worth to note that the complete mineralization of MO in sample SA25 was faster than that of sample SA50. The TiO_2 with 25 mol% SiO_2 exhibited the highest photocatalytic activity, which can be attributed to the combination of several factors including large surface area, high degree of anatase crystallinity, and improved surface acidity. Hence, an optimum amount of SiO_2 (25 mol%) added to TiO_2 systems may be essential to enhance the photocatalytic activity.

Since SA25 was found to be the best sample for MO degradation, this was used to investigate the effect of pH on photocatalytic activity. The $\text{TiO}_2\text{-SiO}_2$ powder prepared at pH 3 and pH 5 showed the highest photocatalytic activity (Figure 10). Rapid degradation rates were observed and resulted in nearly 100% degradation of MO. In contrast, the photocatalytic activity of samples prepared at pH 7, 9, and 12 were very low. Samples from neutral conditions (pH 7) had the anatase structure and high crystallinity, but showed lower photocatalytic activity. As the pH increased from 3 to 7, the crystallite size increased while the surface area decreased, which resulted in lower photocatalytic activity. These observations also indicate that a neutral environment for the synthesis could not enhance the photocatalytic activity. Overall, TiO_2 powder loaded with 25 mol% SiO_2 prepared at pH 3 was the sample with the highest photocatalytic activity.

To investigate the effect of Cu^{2+} on photocatalytic activity, SA25 was loaded with varying amounts of Cu^{2+} . The photocatalytic activity was markedly enhanced in the presence of Cu^{2+} (Figure 11). About 97% of MO was mineralized with the addition of 0.1 mol% of Cu^{2+} . This is mainly due to the high degree of crystallinity of the samples and the capability of Cu^{2+} to induce the formation of new states close to the conduction band, which leads to reduction of the band gap energy and an increase in the photodegradation efficiency. However, as the Cu^{2+} increased, the photocatalytic activity decreased rapidly. The photocatalytic activity dropped to ~21% when the Cu^{2+} content reached 0.5 mol%. This may be attributed to the low crystallinity and the behavior of Cu^{2+} at high concentrations, wherein it becomes a recombination center for the photo-induced electrons and holes thereby inhibits photocatalysis [20]. Hence, an optimum amount of Cu^{2+} in $\text{TiO}_2\text{-SiO}_2$ is essential to improve its photodegradation efficiency.

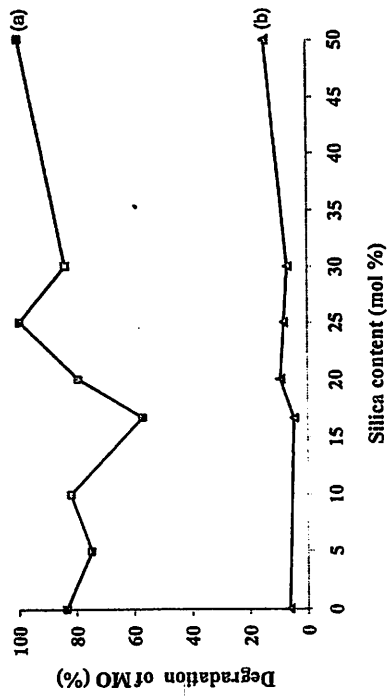


Figure 8 Photodegradation of MO (1 hr) on TiO₂-SiO₂ powder prepared at: (a) pH 3, (b) pH 9.

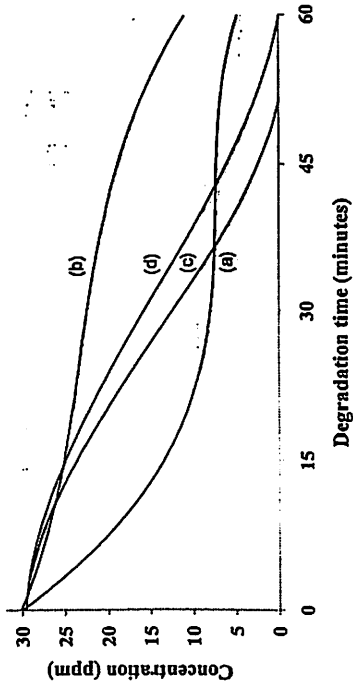


Figure 9 Photodegradation of MO on TiO₂-SiO₂ with various Si content, prepared at pH 3: (a) 0% Si, (b) 16% Si, (c) 25% Si, (d) 50% Si.

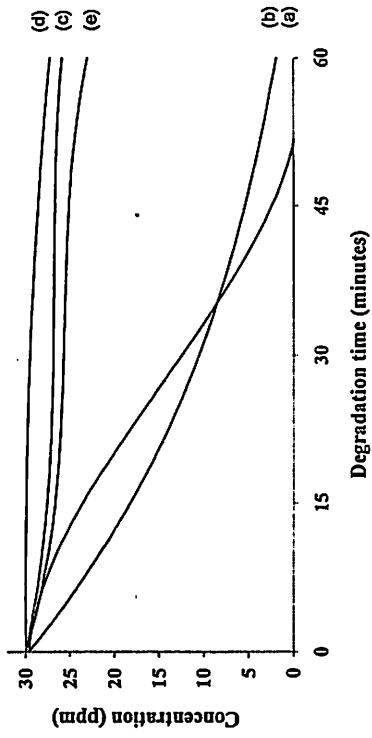


Figure 10 Photodegradation of MO on TiO₂-25 mol% SiO₂ powder prepared at various pH values: a) pH 3, b) pH 5, c) pH 7, d) pH 9, e) pH 12.

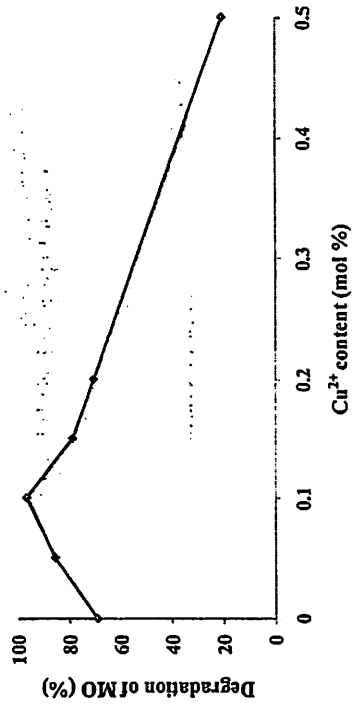


Figure 11 Photodegradation of MO (1 h) on Cu²⁺-loaded TiO₂-25 mol% SiO₂ powder prepared at pH 3.

4.0 Conclusion

The effect of SiO₂ content and pH value on the TiO₂ photocatalytic activity was investigated. Addition of SiO₂ into the TiO₂ strongly affected the degree of crystallinity of the composite. The phase structure was dependent on pH value in the presence of SiO₂. An acidic environment led to anatase phase formation, and samples prepared in basic conditions exhibited the amorphous phase. Addition of SiO₂ improved the surface area of TiO₂ particles by enhancing the surface acidity; this led to high photocatalytic activity compared with pure TiO₂. A higher degree of MO degradation was produced by TiO₂ samples with 25 mol% SiO₂ prepared at pH 3. The TiO₂ loaded with 0.1 mol% Cu²⁺ and 25 mol% SiO₂ exhibited photocatalytic activity higher than that without Cu²⁺. Therefore, the optimum amount of SiO₂ and Cu²⁺ and the pH during preparation were essential to achieving high photocatalytic TiO₂ activity.

Acknowledgments

The authors would like to thank the Universiti Sains Malaysia Fundamental Research Grant Scheme (Grant No. 6071195) and the USM Fellowship for their sponsorship.

References

- [1] S. Kathirvale, M.N. Muhd Yunus, K. Sopian, A.H. Samsuddin, *Renewable Energy*, 29, 559 (2003)
- [2] L.A. Manaf, M.A.A. Samah, N.I.M. Zukki, *Waste Management*, 29, 2902 (2009)
- [3] J.L. Graham, C.B. Almquist, S. Kumar, S. Sidhu, *Catal. Today*, 88, 73 (2003)
- [4] Y. Ide, K. Kashiwabara, S. Okada, T. Mori, M. Hara, *Chemosphere* 32, 189 (1996)
- [5] R. Weber, T. Sakurai, H. Hagenmaier, *Appl. Catal. B: Environmental*, 20, 249 (1999)
- [6] W. Choi, S.J. Hong, Y.S. Chang, Y. Cho, *Environ. Sci. Technol.* 34, 4810 (2000)
- [7] A.L. Linsebigler, G. Lu, J.T. Yates Jr., *Chem. Rev.* 95, 735 (1995)
- [8] K. Hashimoto, H. Irie, A. Fujishima, *Jpn. J. Appl. Phys.* 44, 8269 (2005)
- [9] X. Chen, S.S. Mao, *Chem. Rev.* 107, 2891 (2007)
- [10] X. Chen, *Chin. J. Catal.* 30, 839 (2009)
- [11] M. Bellardita, M. Addamo, A. Di Paola, G. Marci, L. Palmisano, L. Gassar, M. Borsa, *J. Hazardous Materials* 174, 707 (2010)
- [12] J. Bennani, R. Dillert, T.M. Gessing, D. Bahnemann, *Separation and Purification Technology* 67, 173 (2009)
- [13] Y. Arai, K. Tanaka, A.L. Khlaifat, *J. Mol. Catal. A* 243, 85 (2006)
- [14] R.A. Aziz, I. Sopyan, *Indian J. Chem.* 48, 951 (2009)
- [15] R.N. Viswanath, S. Ramasamy, *Colloids and Surfaces. A* 133, 49 (1998)
- [16] K.Y. Jung, S.B. Park, *Mater. Lett.* 58, 2897 (2004)

- [17] S.R. Kumar, C. Suresh, A.K. Vasudevan, N.R. Suja, P. Mukundan, K.G.K. Warriar, *Mater. Lett.* 38, 161 (1999)
- [18] R.F. Chen, C.X. Zhang, J. Deng, G.Q. Song, *Int. J. Minerals, Metallurgy and Materials* 16, 220 (2009)
- [19] H. Chun, T. Yuchao, T. Hongxiao, *Catal. Today*. 90, 325 (2004)
- [20] D. Zhang, *Transition Met. Chem.* 35, 933 (2010)
- [21] C.H. Kwon, J.H. Kim, I.S. Jung, H. Shin, K.H. Yoon K H, *Ceram. Inter.* 29, 851 (2003)
- [22] L.Zhou, S. Yan, B. Tian, J. Zhang, M. Anpo, *Mater. Lett.* 60, 396 (2006)
- [23] J.G. Yu, J.C. Yu, X. Zhao, *J. Sol-Gel Sci.* 24, 95 (2002)
- [24] G. Xu, Z. Zheng, Y. Wu, N. Feng N, *Ceram. Inter.* 35, 1 (2009)
- [25] P. Cheng, M. Zheng, Y. Jin, Q. Huang, M. Gu, *Mater. Lett.* 57, 2989 (2003)
- [26] Z. Li, B. Hou, Y. Xu, D. Wu, Y. Sun, W. Hu, F. Deng F, *J. Solid State Chem.* 178, 1395 (2005)
- [27] M.Hirano, K. Ota, *J. Am. Ceram. Soc.* 87, 1567 (2004)
- [28] J.G. Yu, Y. Su, B. Cheng, M. Zhou, *J. Mol. Catal. A* 258, 104 (2006)
- [29] A. Karami, J. Iran, *Chem. Soc.* 7, 154 (2010)
- [30] K. Guan, B. Lu, Y. Yin, *Surface and Coating Technology* 173, 219 (2003)
- [31] J.G. Yu, H. Yu, B. Cheng, C. Trapalis, *J. Mol. Catal. A* 249, 135 (2006)
- [32] J.G. Yu, H. Yu, B. Cheng, X. Zhao, Q. Zhang, *J. Photochem. Photobiol. A* 182, 121 (2006)

- [33] Y.Q. Wang, G.Q. Hu, X.F. Duan, H.L. Sun, Q.K. Xue, *Chem. Phys. Lett.* 365, 427 (2002)
- [34] K. Guan, *Surface and Coating Technology* 191, 155 (2005)

Purchase Requisition		Purchase Order		Suppliers		Maintenance		Financials		Coda Info		Reports		Admin	
UserCode: HAIZAN / USMKCLIVE / PBAHAN				Program Code: Votebook9100				Current Program : Votebook (Header)							
Current Date : 26/08/2011 11:13:39 AM				Version: 13.92, Last Updated at 30/05/2011				DB: 13.00, 09/18/2010 VB: 13.01, 03/14/2011				Switch Language : English /Malay			
Wildcard : eg. Like 100%, Like 10%1, Like %1															
Element 1:		<input type="text"/>		Element 2:		<input type="text" value="%"/>		Element 4:		<input type="text" value="PBAHAN"/>		<input type="text"/>		<input type="text"/>	
Element 5:		<input type="text" value="6071195"/>		Year:		<input type="text" value="2011"/>									
Detail	Excel	Budget Rule	Budget Control	Account Description	Budget Account Code	Roll over	Budget	Cash Received	Advanced	Commit	Actual	Available	Percentage		
Detail	Excel	116	T	Penyelidikan Fundamentals (FGRS)	203.111.0.PBAHAN.6071195	3,859.95	0.00	0.00	0.00	0.00	0.00	3,859.95	0.00%		
		116	T	SubTotal		3,859.95	0.00	0.00	0.00	0.00	0.00	3,859.95	0.00%		
Detail	Excel	117	T	Penyelidikan Fundamentals (FGRS)	203.221.0.PBAHAN.6071195	-532.00	0.00	0.00	0.00	0.00	0.00	-532.00	0.00%		
Detail	Excel	117	T	Penyelidikan Fundamentals (FGRS)	203.227.0.PBAHAN.6071195	-3,892.40	0.00	0.00	0.00	6,378.50	5,244.00	-15,514.90	0.00%		
Detail	Excel	117	T	Penyelidikan Fundamentals (FGRS)	203.229.0.PBAHAN.6071195	4,870.42	0.00	0.00	0.00	0.00	450.00	4,420.42	0.00%		
		117	T	SubTotal		446.02	0.00	0.00	0.00	6,378.50	5,694.00	-11,626.48	0.00%		
		9999		GrandTotal		4,305.97	0.00	0.00	0.00	6,378.50	5,694.00	-7,766.53	0.00%		

Appendix C

Technical Report

Final Technical Report FRGS (1 Mei 2010-Aug 2011)

Introduction

Titanium (Ti) and its alloys have been widely used as important biomaterials for many years. In particular, Ti-6Al-4V is widely used as a biomaterial for artificial hip or dental implants because of its special mechanical, chemical and biological properties. It can provide direct physical bonding with adjacent bone surface without forming a fibrous tissue interface layer. Although the success rates of implant are very high, implants occasionally loosen and fail. Pure Ti metal lacks desirable bioactive (bone-growth) properties, a thin TiO_2 passivation layer forms on Ti surface to impart bioactivity and chemical bonding to bone. Such a layer, however, is composed of smooth and dense TiO_2 layer and is susceptible to the formation of fibrous tissue that prohibits osteoblastic cells from firmly attaching onto the surface, and can cause the loosening of implant and inflammation (Yu et al., 2010). Thus surface modifications, altering topography and chemical composition of these materials, are required to enhance direct structural and functional anchoring of the prosthesis to the living bone (osseointegration). The most common surface treatments of commercially available implants and prosthesis encompass pickling, sandblasting, plasma spraying, anodizing, and micro-arc oxidation. For decades, until recently, cell interactions and bone response were studied on implant surfaces with micrometer-scale topography. It have shown that nanoscale topography as well as the order of the nanofeatures organisation is a critical factor romoting early cell responses to the implant surface (Das et al., 2009). Hence the fabrication of highly ordered TiO_2 nanotube films for biomedical applications is attracting much attention. Among these processes, electrochemical anodization of titanium in fluorinated electrolytes is a relatively simple method to synthesize porous or tubular structures. In this work, anodization process was performed in ethylene glycol containing fluoride and de-ionized water to produce the nanotubes structure. Then heat treatment was conducted to produce various crystalline structure which are anatase and rutile phase of TiO_2 . The final stage was on testing the cell interaction on the different crystallines TiO_2 nanotubes.

Problem statement

Ti-6Al-4V alloys possessed two-phase of alpha and beta structures which are aluminum and vanadium, respectively. It has been reported that this alloy associated with long term health problem due to toxicity of aluminum and vanadium released. Titanium based alloy tends to undergo severe wear when rubbed with other metals, it is also stated that the two-phase equiaxed microstructure more susceptible to corrosion as the compositional difference across the grain boundaries increases which leads to the galvanic cell formation (Geetha et al., 2009). Thus, surface treatment modification such as formation of thick TiO_2 nanotubes that protects the surface of implants as well as giving good adhesion with cell has been applied on titanium and titanium alloys to increase the longevity of implant. Surface microstructure is an important factor in modulating cell response at the implant/bone interface. In the formation of TiO_2 nanotubes highly dependent on the electrolyte composition and electrochemical conditions. There are not many literatures reports on the formation of TiO_2 nanotubes of Ti alloys in organic electrolytes especially in ethylene glycol. It is anticipated that if the morphology is well defined, the cell interaction study will be improved due to the improvement of the interaction of nanotubes with cells. Therefore in this work comprehensive investigation on the formation of nanotubes on Ti alloy was reported.

Objectives of this project

The objectives of this research are as follows:

- To grow TiO₂ nanotubes on Ti-6Al-4V alloy via anodization method.
- To study the effect of NH₄F content, applied voltage, and anodization time on the formation of TiO₂ nanotubes on Ti-6Al-4V alloy.
- To characterize crystal structure phase and morphology of TiO₂ nanotubes.
- To study the response of human foreskin fibroblast (HS27) cell on optimized TiO₂ nanotubes with different crystalline structure.

Results and Discussions

Morphology of Ti-6Al-4V

Prior to anodization experiment, Ti alloy sheet was chemically cleaned by solution of 1 M HNO₃ and 0.45 M NH₄F to remove native oxide layer on the surface of Ti-6Al-4V. Figure 1 shows FESEM images of Ti-6Al-4V after the cleaning process. As seen, the surface of the Ti alloy is rough and irregular with two different distinct regions. Certain region composed of small grain while the others are large. EDX analysis was used to test the difference within this two regions and it was found the small grains are enriched with V while the big grains are composed of Al.

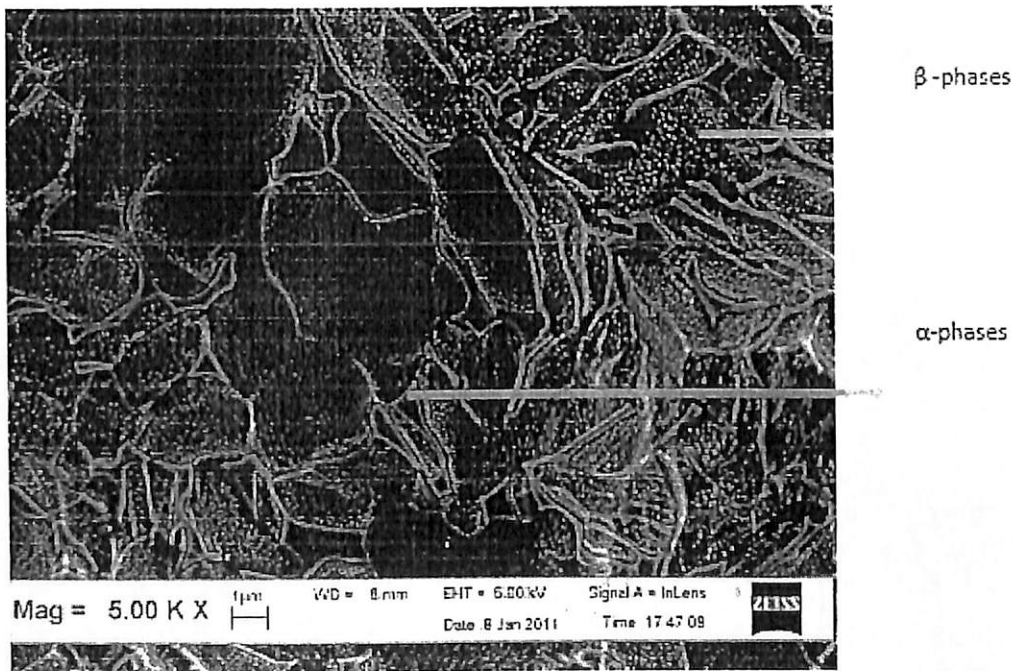


Figure 1: FESEM image showing the Ti6Al4V alloy sheet of after the cleaning process (α and β phases are an-noted with arrows; α -phases are dark; β -phases are bright). The image acquired after ultrasonically cleaned in 1M HNO₃ and 0.45 M NH₄F for 1 minute. The β phases are enriched in V.

Anodization of Ti-6Al-4V in ethylene glycol

Effect of NH₄F content on the anodization of Ti alloys in ethylene glycol

In this part, the experiment was conducted to investigate the effect of different amount of NH₄F on the morphologies of the nanotubes. Hence optimum weight of NH₄F to produce self organized nanotubes can be determined. All samples are anodized in 99 ml

ethylene glycol and 1 ml H₂O at 60V for 1 hour and were annealed at 400 °C. This parameter was selected based on our preliminary studies (Sreekantan et al., 2010). The content of NH₄F was varied from 0.1 g, 0.3 g, 0.5 g and 0.7 g. The surface morphology of Ti-6Al-4V sheet anodized in ethylene glycol with different fluoride content lead to different morphologies (Figure 2). Anodization of Ti alloy in electrolyte containing 0.1g NH₄F gives an irregular nanoporous structure (Figure 2a). There are areas covered with small pits while other have larger pores. The pits or pores are formed due to the different in the degree of localized dissolution of the oxide layer. (Figure 2b) shows the Ti alloys anodized at 0.3 g NH₄F. As seen the pit and pores which are seen for 0.1 g NH₄F have been converted into sponge like structure. The inset shows length of sponge like structures of about 163.8 nm. It could also be found that the entire metallic surface was not uniformly covered with nanoporous structure.

For 0.5 g and 0.7 g NH₄F, self organized TiO₂ nanotubes array is formed (Figure 2 c and d). The average diameter of the nanotubes is approximately 81 and 110 nm for 0.5 g and for 0.7 g, respectively. Generally the pores or the nanotube diameter are found to be larger with increasing fluoride content in the electrolyte. This is due to enhanced chemical dissolution makes the barrier layer at the bottom relatively thin, which in turn lead to easier transport of the fluoride ions in oxide layer. Such condition increases the electrical field intensity resulting in further pore or nanotube growth.

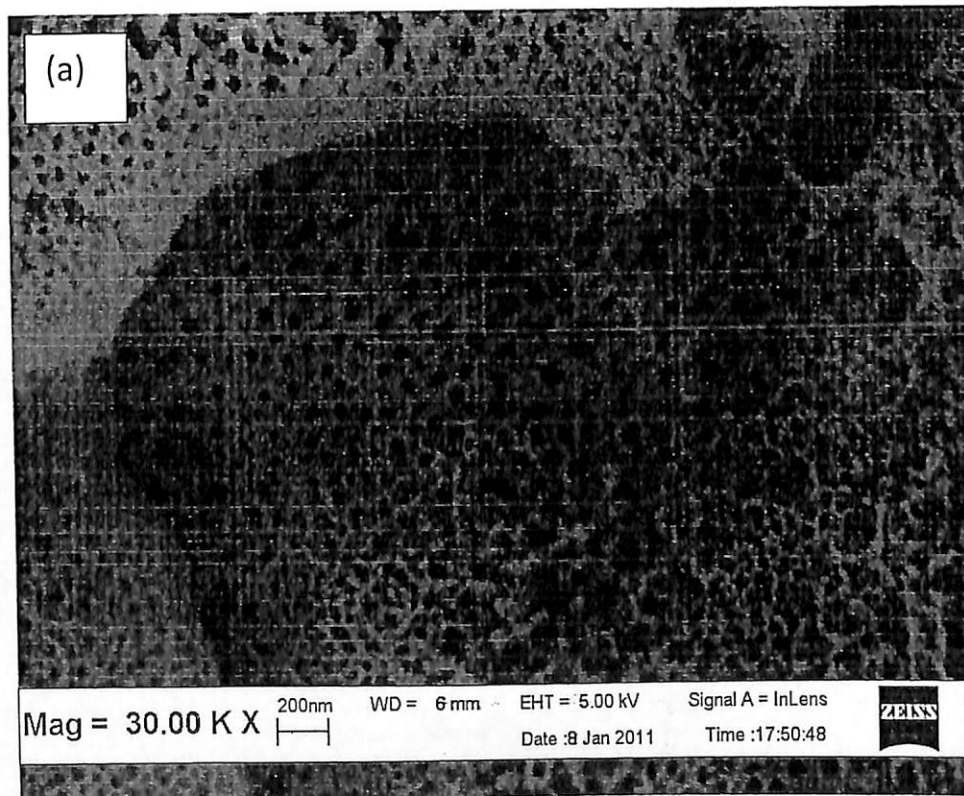


Figure 2(a): FESEM images of TiO₂ nanotubes anodized in 99 ml ethylene glycol + 1 ml H₂O with 0.1 g NH₄F, at 60V for 60 minutes.

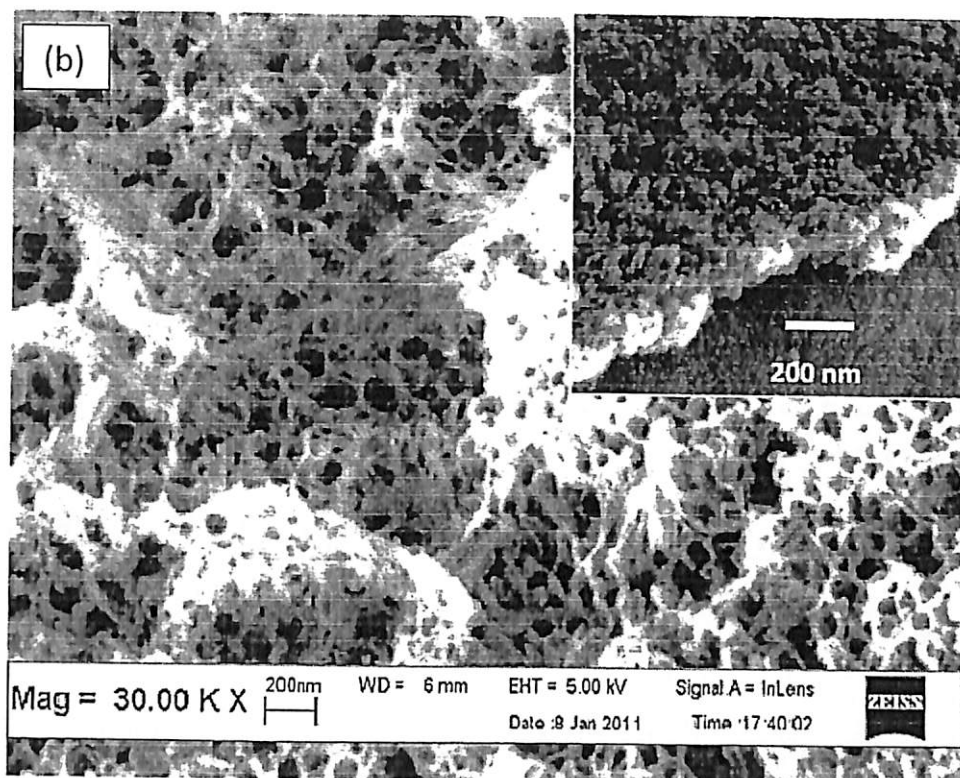


Figure 2(b): FESEM images of TiO_2 nanotubes anodized in 99 ml ethylene glycol + 1 ml H_2O with 0.3g of NH_4F , at 60V for 60 minutes. Inset shows the cross sectional view.

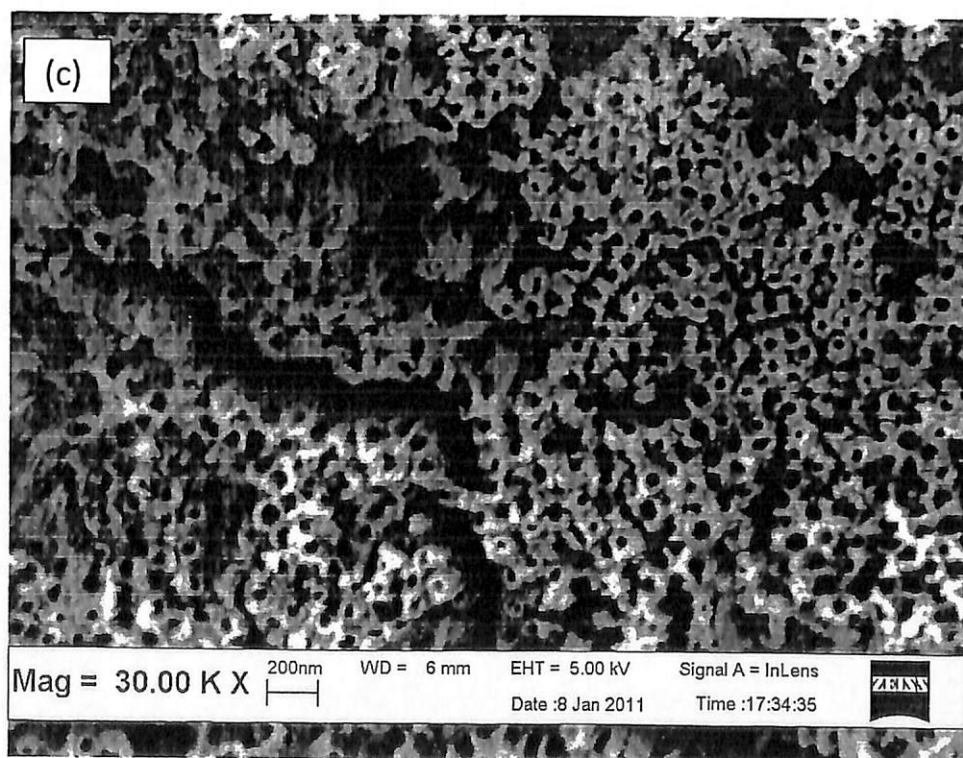


Figure 2(c): FESEM images of TiO_2 nanotubes anodized in 99 ml ethylene glycol + 1 ml H_2O with 0.5 g of NH_4F , at 60V for 60 minutes.

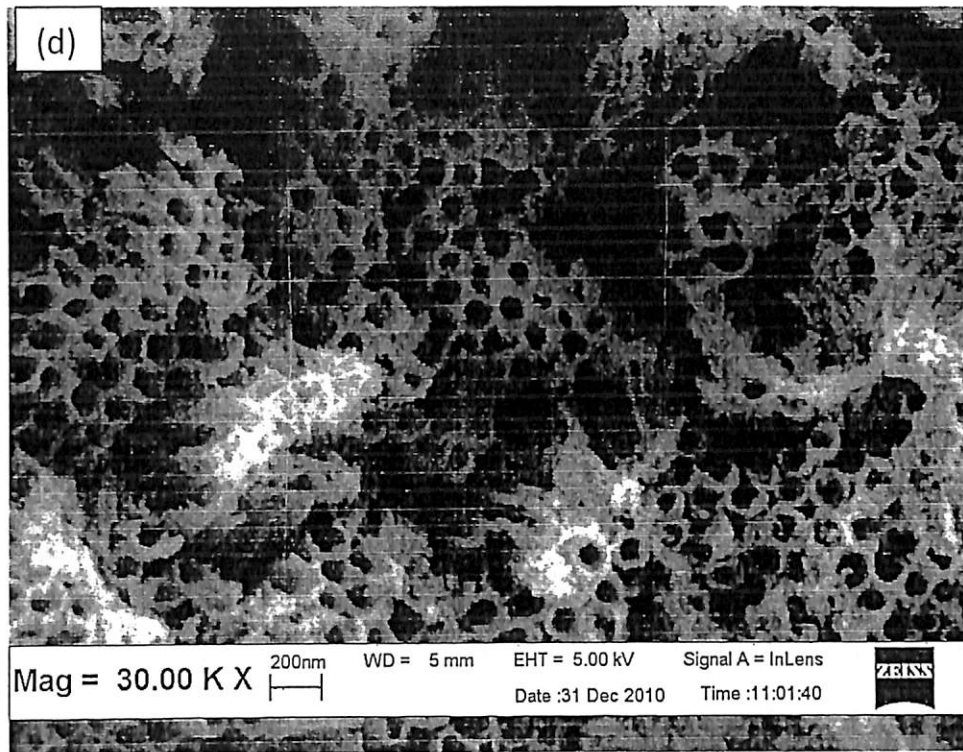


Figure 2(d): FESEM images of TiO₂ nanotubes anodized in 99 ml ethylene glycol + 1 ml H₂O with 0.7 g of NH₄F, at 60V for 60 minutes.

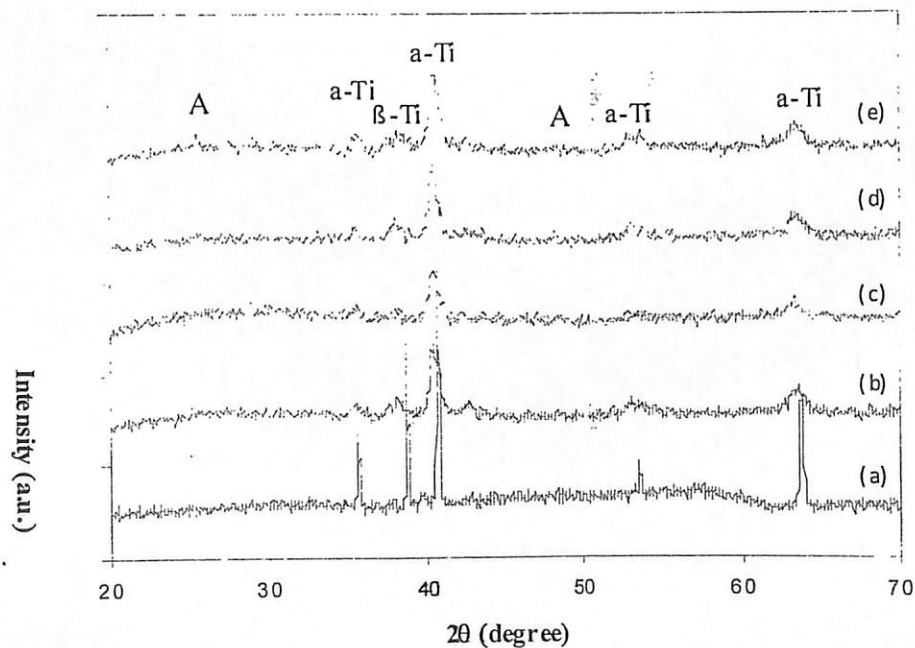


Figure 3: XRD pattern of the annealed Ti-6Al-4V alloy sheets anodized in EG at 60V for 60 minutes with (a) as-anodized at 30 V (b) 0.1 g, (c) 0.3 g, (d) 0.5 g, and (e) 0.7 g weight of NH₄F. A = Anatase, α -Ti = alpha Ti and β -Ti = Beta Ti.

The corresponding XRD pattern of the Ti alloy sheet anodized in 0.1 g, 0.3 g, 0.5 g and 0.7 g NH_4F is shown in Figure 3. After annealing at 400 °C, the diffraction peak appears at 2θ of 25° representing (101) plane of anatase TiO_2 . In addition, diffraction pattern of α -Ti at $2\theta = 35.18^\circ, 40.26^\circ, 53.08^\circ$ and 63.19° corresponding to the (100), (101), (102), (110) plane and β -Ti peak at 38.75° corresponding at (002) plane were detected. These peaks are originated from the substrate of the Ti alloy. It is worth nothing the peak intensity of α and β Ti decreased as the content of fluoride increased. This is likely due to larger thickness of the oxide layer formed on the Ti alloy.

Effect of voltage on anodization of Ti alloy in ethylene glycol

Experiment was continued in similar electrolyte with 0.7 g NH_4F to investigate the effect of voltage on the Ti alloy. The voltage was varied from 10 V, 20 V, 30 V, 40 V, and 60 V for 1 hour. Different voltage in anodization process leads to different surface structure of TiO_2 . At low anodization voltage (10V) in Figure 4a, small pits are observed on the surface of the oxide layer. At this stage the dissolution of titanium had just occurred. As the voltage increased to 20 V in Figure 4b, the pits nucleate to form large porous structure. However, not all the surface is covered with porous TiO_2 . There are still areas covered with oxide layer. This is due to the insufficient voltage to induce complete dissolution and breakdown of barrier layers to dissolve the oxide into tubes.

When voltage increased to 30V up to 60V, self organized nanotube arrays are formed. However the lengths of the nanotubes in certain area are relatively low as compared to others (insets in Figure 4c). This finding is different compared to few authors who claimed the existence of two kinds of the nanostructure on the surface of the Ti alloy. One was self organized nanotube arrays and the other was irregular nanoporous structure. According to few authors (Luo et al., 2008 and Matykinaa et al., 2011), the self organized nanotubes arrays are proven to be grown on the α phase region and nanoporous structure on β phase region. The α phase are enriched with Al whereas β phase region enriched with V. Because of the different chemistries of these phases, the formation of the nanotubular oxide layer is not uniform as β phases get etched preferentially by the electrolyte. Different results were obtained in this work probably due to different electrolyte used. Most of the aforementioned studies utilize aqueous solution which subjected high chemical dissolution rate. In here the use of ethylene glycol with pH 6.5 could avoid the significant attack on β phase and produce homogeneous microstructure. However, the length of the nanotubes are different within the α and β phase region, being short at β phase region as the solubility of V is faster than the Al.

The average diameter and the length of the nanotubes formed with various anodization voltages are shown in Figure 5. Generally it was found that raising the applied voltage leads to larger diameter and length. This is due to the high applied electric field which leads to enhance polarization of Ti-O bond and thus weakened to promote dissolution of the metal oxide. This lead to greater driving force for ionic transport through the barrier layer at the bottom of the nanotubes favouring formation of $[\text{TiF}_6]^{2-}$ complex that will eventually accelerate the pore growth. At the same time, the faster movement of the Ti/ TiO_2 interface into the metal (Shankar et. al, 2007) resulted in the formation of long nanotubes. The standard deviation of nanotube diameter at different voltages is almost constant, in the range of (5-10nm) but for length showed significant difference due to high solubility of V which reduces the length of the nanotubes in certain region. The side view of the nanotubes is relatively smooth as seen in Figure 6. However, TEM analysis showed the presence of small ridges at the wall. It is also found that the nanotubes are uniform with hollow nature of tube opening. The thickness of the wall was approximately 20 nm.

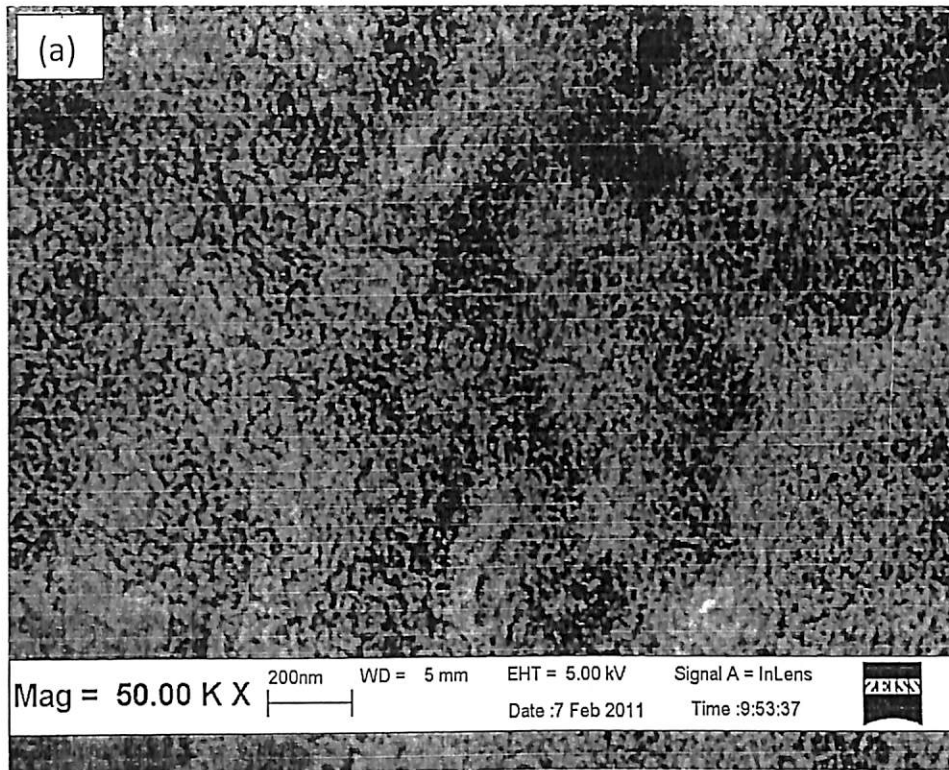


Figure 4(a): FESEM images of TiO_2 nanotubes anodized in 99 ml ethylene glycol + 1 ml H_2O + 0.7 g NH_4F for 60 minutes at 10 V.

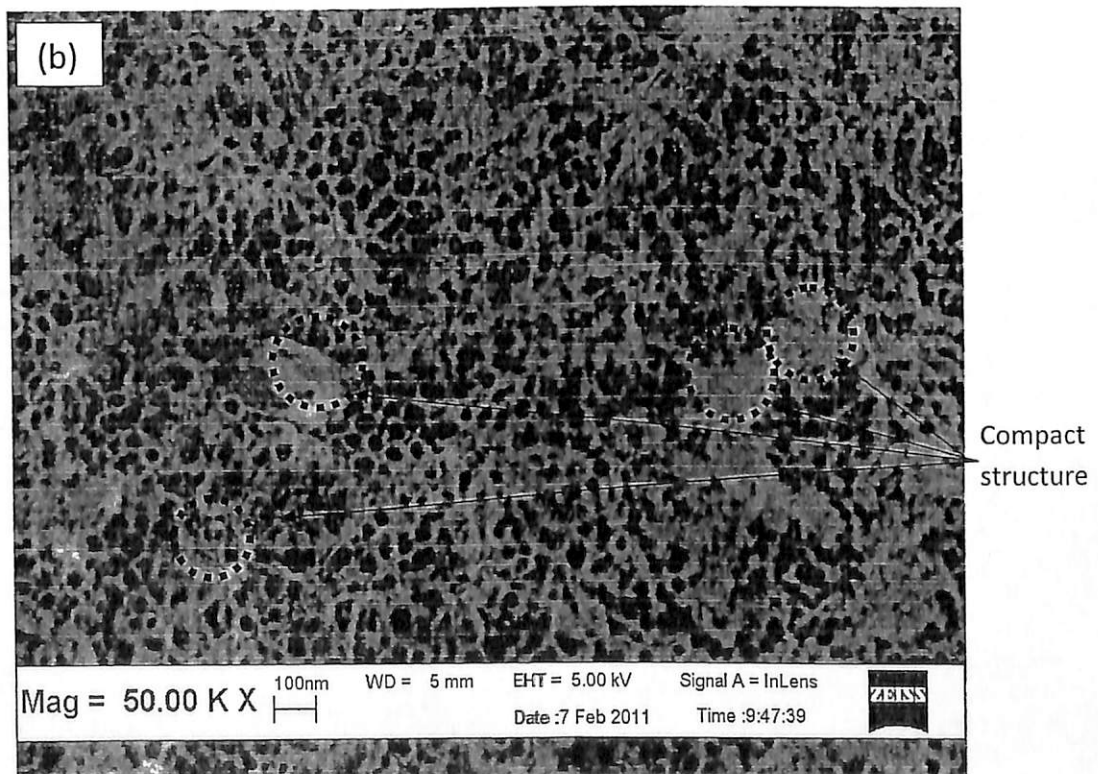


Figure 4(b): FESEM images of TiO_2 nanotubes anodized in 99 ml ethylene glycol + 1 ml H_2O + 0.7 g NH_4F for 60 minutes at 20 V.

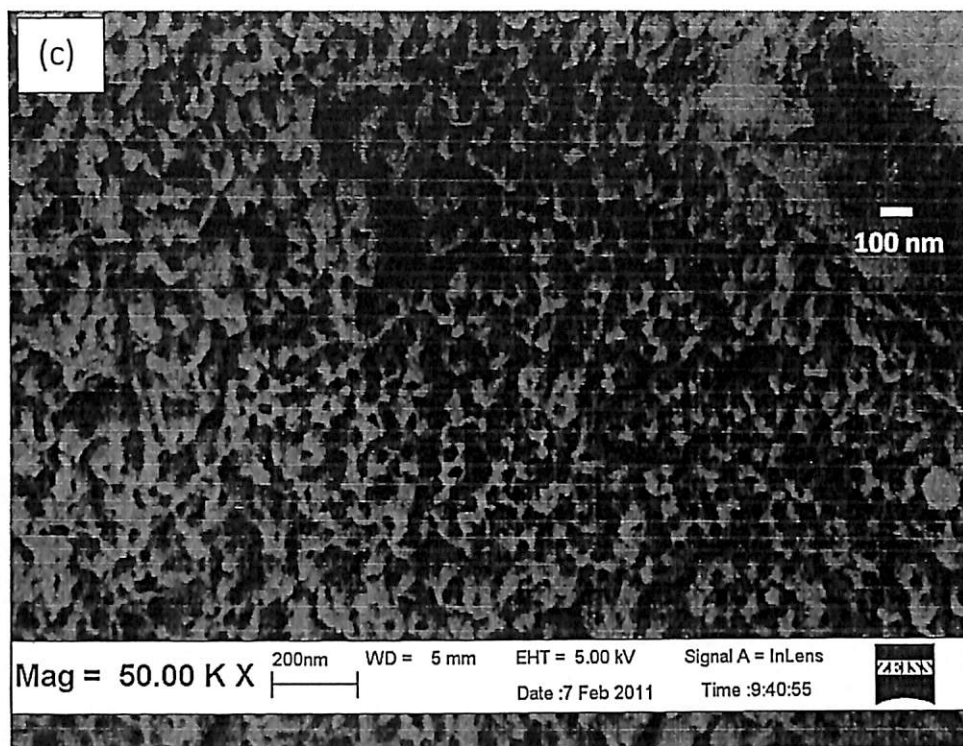


Figure 4(c): FESEM images of TiO_2 nanotubes anodized in 99 ml ethylene glycol + 1 ml H_2O + 0.7 g NH_4F for 60 minutes at 30 V. Inset shows the cross sectional view.

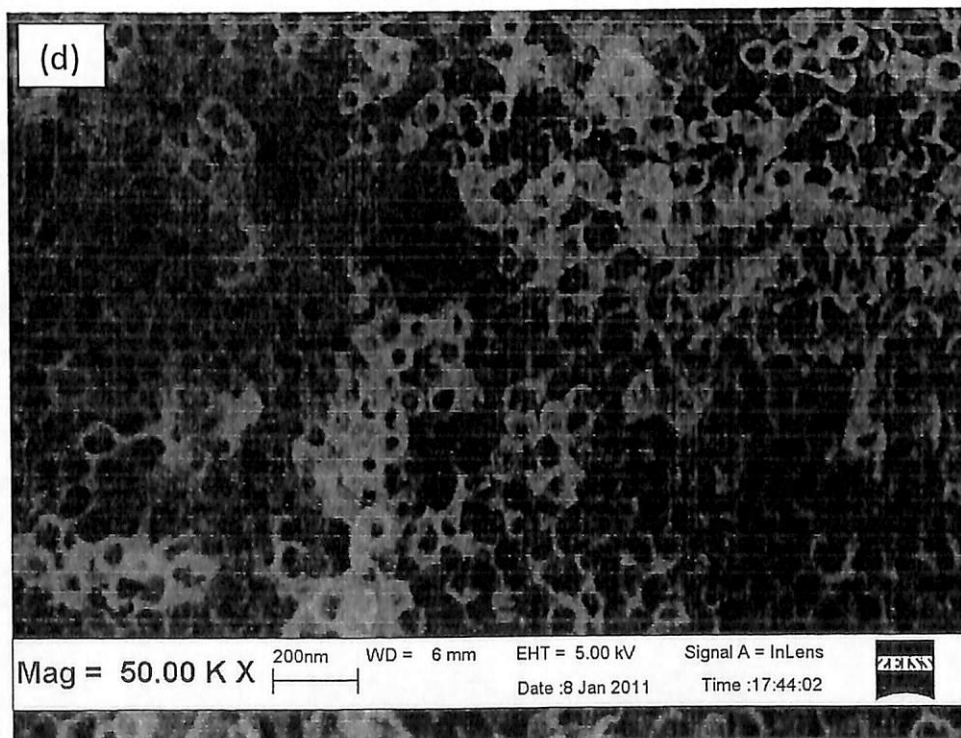


Figure 4(d): FESEM images of TiO_2 nanotubes anodized in 99 ml ethylene glycol + 1 ml H_2O + 0.7 g NH_4F for 60 minutes at 40 V.

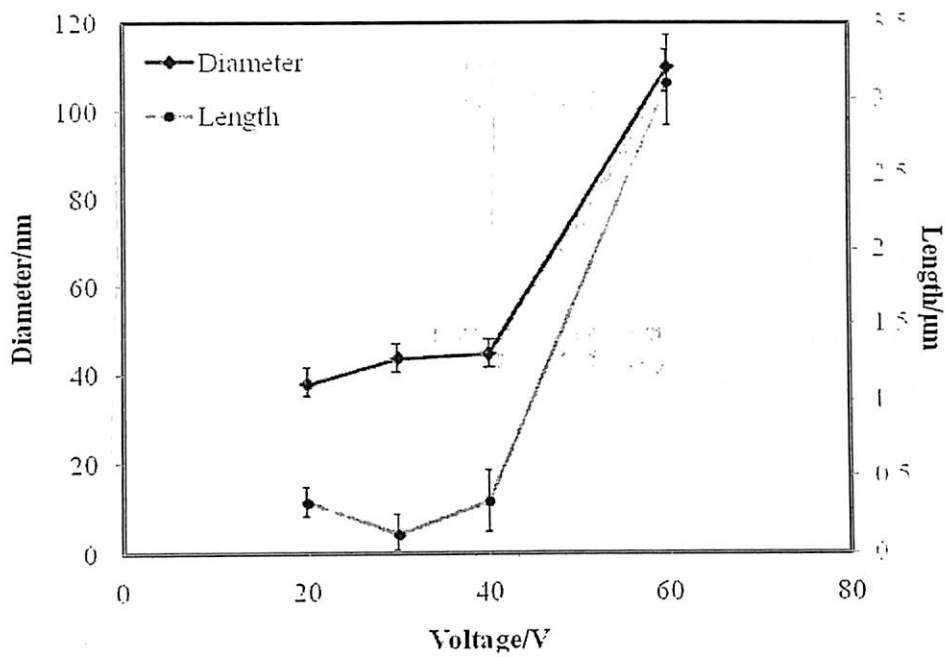


Figure 5: Variation in the pore diameter and length of compact/ nanotube structure prepared as a function of voltage

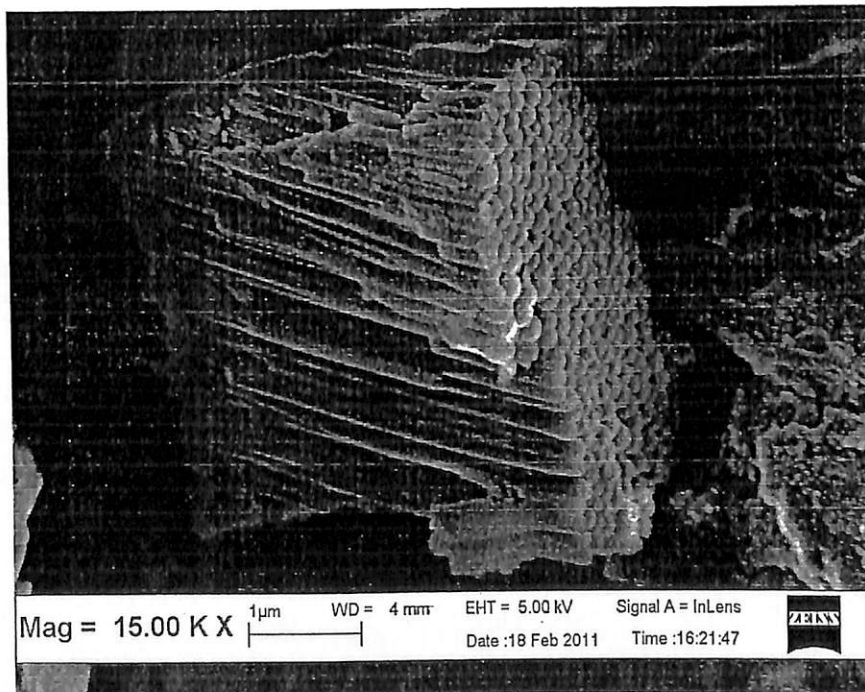


Figure 6: FESEM image of side view with TiO_2 nanotubes

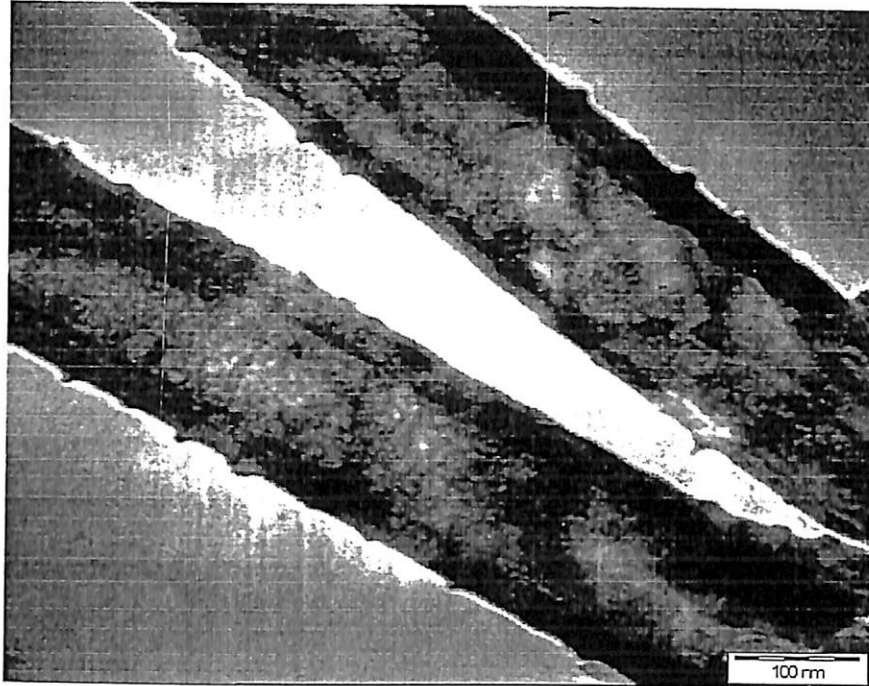


Figure 7: TEM image of small ridges found at the wall of nanotubes.

c:\edax32\genesis\genmaps.spc 07-Feb-2011 10:53:22
LSecs : 101

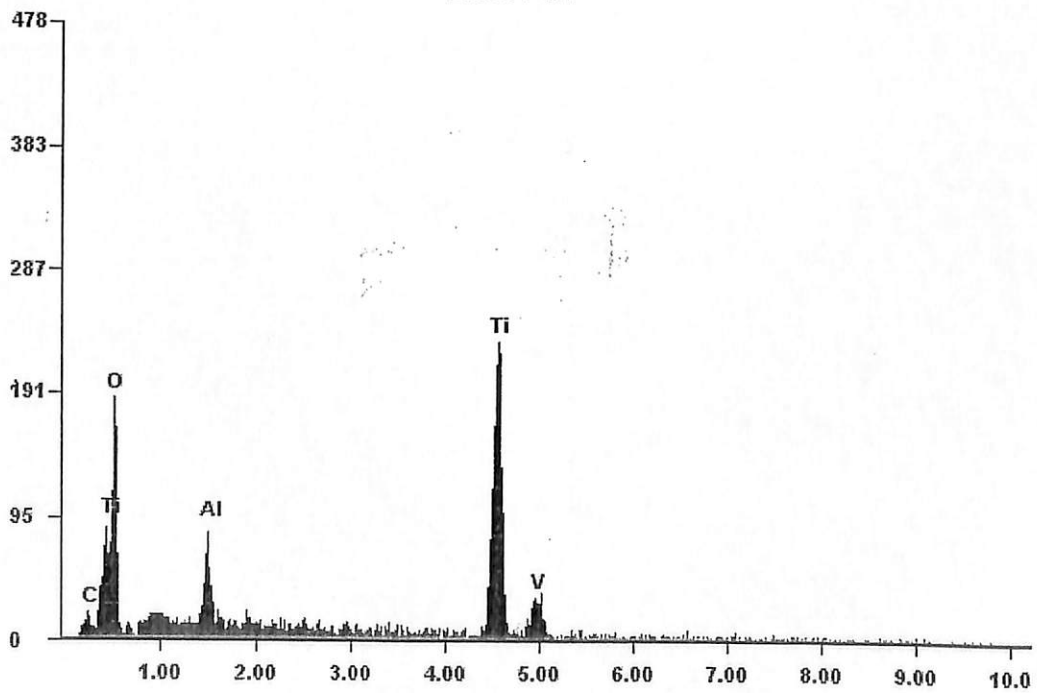


Figure 8: EDX spectra of the oxide residual found on the Ti alloy surface after anodized in 99 ml ethylene glycol + 1 ml H₂O + 0.7 g NH₄F, at 40 V

The chemical composition of the TiO₂ nanotubes prepared at various voltages was determined using EDX analysis. The representative spectrum of the Ti alloy anodized at various voltages is shown in Figure 8. The result clearly shows the presence of C, O, Al, Ti and V. EDX spectrum of the other sample are almost similar (not shown), only slight variation on the At % of all the elements. However it is interesting to note that the composition of the vanadium slightly reduced from 2.3% to 1.76 % with increase voltage from 10 to 60 V. This is probably due to preferential etching of V at high voltage as compared to other phases.

Table 4.1: EDX spectrum at various voltages.

Element	At % at different voltage		
	10 V	40 V	60 V
C	03.42	05.13	04.58
O	47.10	39.86	43.68
Al	04.68	05.50	04.19
Ti	39.53	44.20	42.77
V	02.30	02.16	01.76

X-ray Photoelectron Spectroscopy (XPS)

The chemical composition present at the surface of Ti-6Al-4V nanotube subjected to annealing at 400 °C for 4 hours under Argon atmosphere was investigated using XPS analysis, and the result is shown in Figure 9. Based on the result, the binding energies of Ti2p_{3/2} and Ti2p_{1/2} were found at 456.5 eV and 463.3 eV, respectively (Figure 9a). This is likely due to the presence of Ti⁴⁺ oxidation state. The Ti⁴⁺ ions reacted with O²⁻ ions during anodization, and consequently formed TiO₂. This was confirmed by the presence of Ti-O (527.5-527.7 eV) in O1s (Figure 9b). Besides, the presence of OH⁻ ions and absorbed H₂O was detected at 528.9 eV and 531.9 eV. Other than the information of TiO₂, binding energy of Al2p was traced at 72.1 eV, 72.2 eV and 73.9 eV (Figure 9c). This is attributed to the binding energy of Al-O, which is in agreement with that report by Li et al, (2008). In addition, the V2p_{3/2} peak corresponding to the metallic V appears at 515.5 eV and 518.2 eV (Figure 9d). This is due to the fact that the affinity of Al and Ti with O is stronger than that of V. Al and Ti diffused outward, bringing on implanted layer outward growing, therefore V is deficient relatively in the outmost layer. However, the existing of oxidized state of Al, and the leaching of V contribute to the reduce cellular toxicity of Al and V of Ti-6Al-4V as biomaterial (Li et al., 2008).

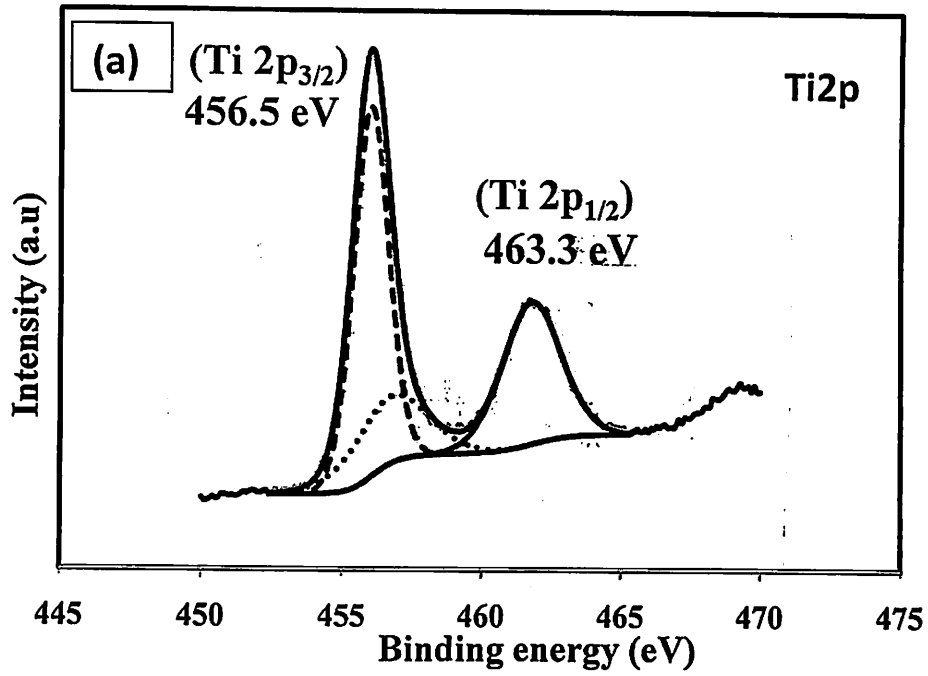


Figure 9(a): XPS spectra of Ti2p region

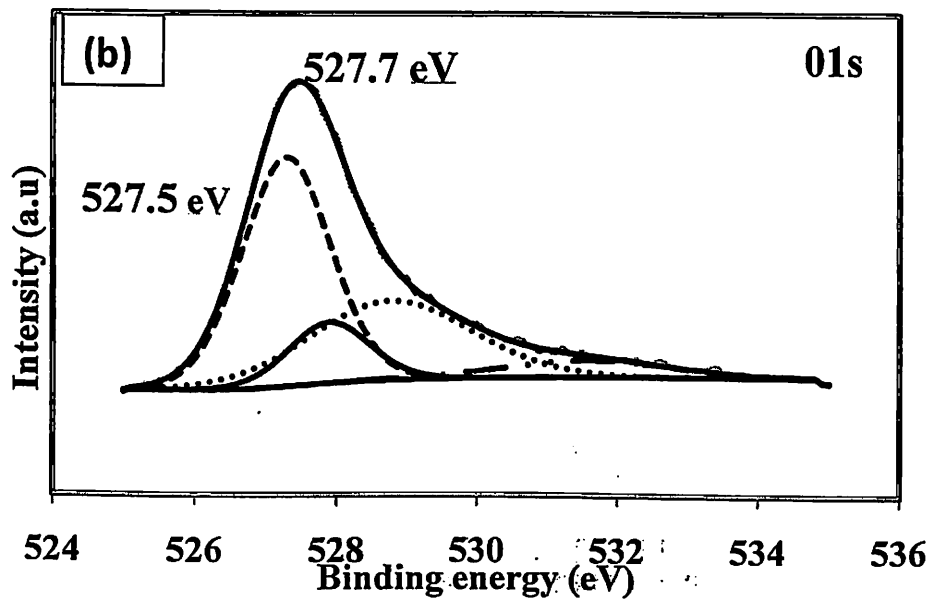


Figure 9 (b): XPS spectra of O1s region

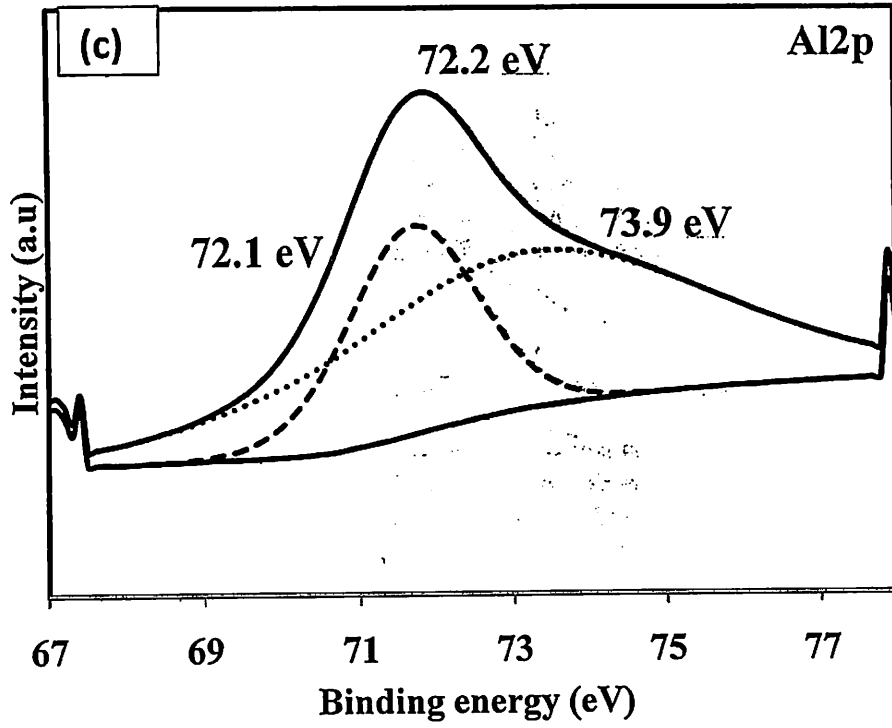


Figure 9(c): XPS spectra of Al₂p region

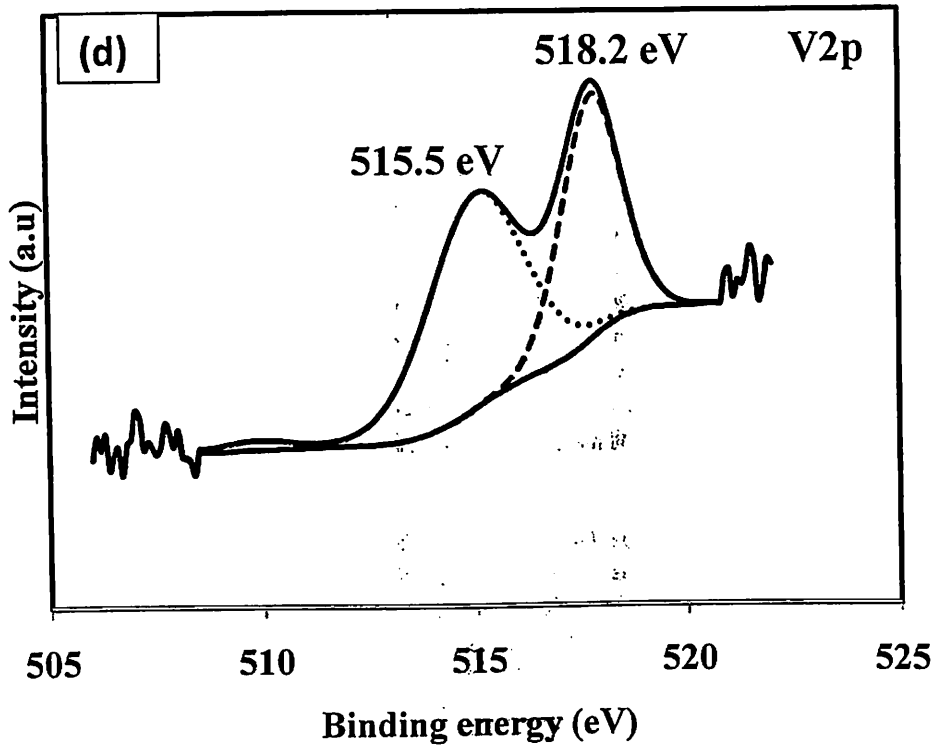


Figure 9(d): XPS spectra of V₂p region

Effect of anodization time on anodized Ti alloys in ethylene glycol

This set of experiments was done to monitor the growth of nanotubes with increasing anodization time. The experiment was carried out in similar electrolyte with 0.7 g F at 60V. The growth of the nanotubes was monitored by taking FESEM images of various time intervals (20 seconds, 1 minute, 5 minutes, 10 minutes, 15 minutes, 30 minutes, 1 hour and 6 hours). Table 4.2 shows the diameter and length of nanotubes, Ti-6Al-4V alloy formed in the variation of anodization time.

Table 4.2: Diameter and Length of TiO₂ nanotubes in different anodization time

Time (minutes)	Tube Diameter (nm)	Tube Length (μm)	Morphology
20 sec	-	-	Compact structure
1	-	0.4	Pits formation
5	64	1.4	Porous structure
10	68	1.7	nanotubes
15	70	1.6	nanotubes
30	100	2.8	nanotubes
1 hour	110	3.1	nanotubes
6 hours	159	6.4	nanotubes

Figure 10a shows the image of the surface of 20 seconds. An oxide layers are formed on the surface of the of Ti alloy due to the interaction within O²⁻ and OH⁻. After 1 minute the oxide layer has been etched in certain area, thus forming irregular pits due to localized dissolution (Figure 10b). After 5 minutes of anodization, the pits are converted to larger pores (Figure 10c). However most of the areas are still covered with oxide layer. At 10 minutes, the pore density is increased and the cross sectional view (Figure 10d) confirms the formation of nanotube structure. After 15 minutes, the surface is completely filled with self organized nanotubes arrays (Figure 10e). Prolonging the anodization time to 30 minutes (Figure 10f), 1 hour (Figure 2d) and 6 hours (Figure 10g) resulted in larger diameter and tube length. The overall formation of the nanotubes on Ti alloy (Ti-6Al-4V) is similar to the Ti-8Mn reported by Mohapatra et al.

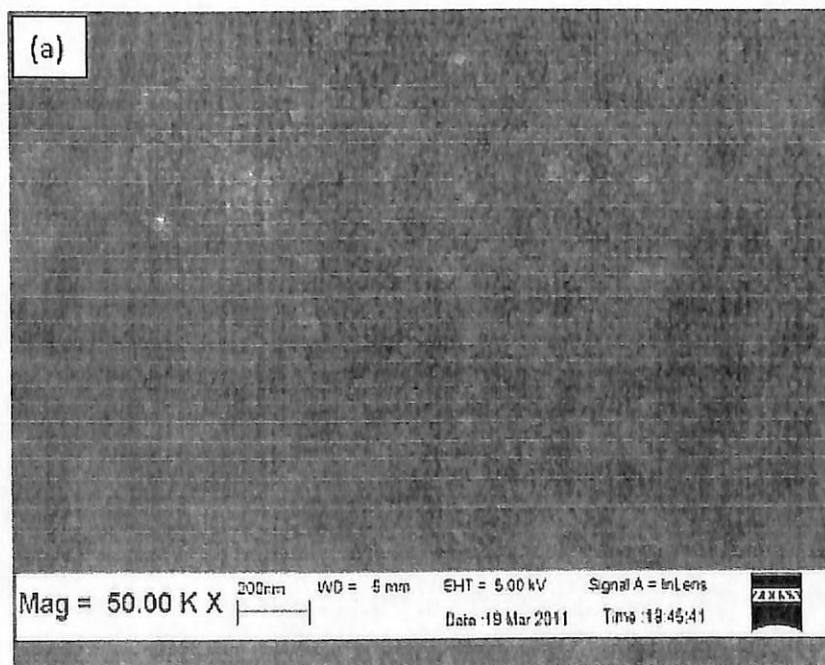


Figure 10a: Top view of FESEM images of TiO₂ nanotubes anodized at 20 seconds.

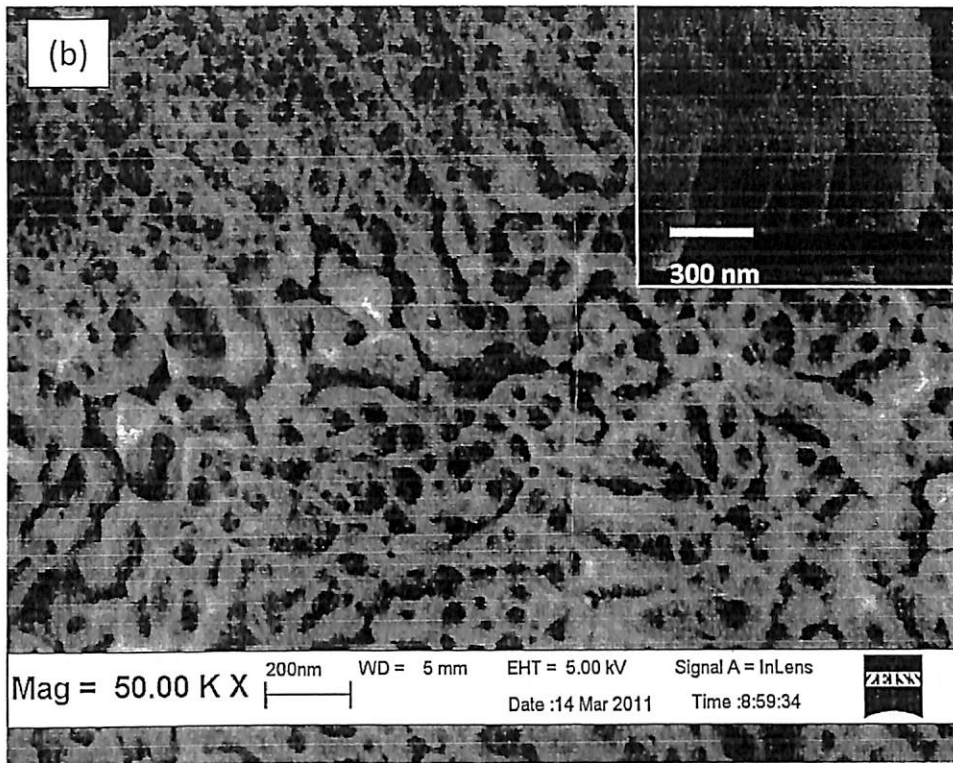


Figure 10b: Top view of FESEM images of TiO_2 nanotubes anodized at 1 minute. The inset shows cross sectional view of the sample

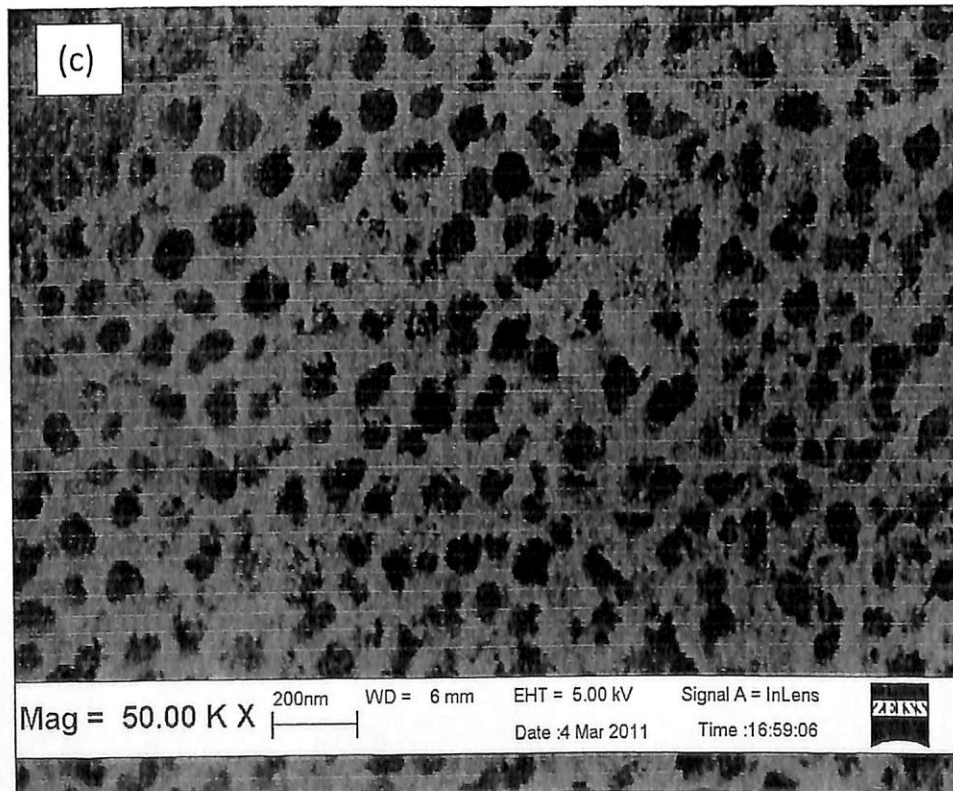


Figure 10c: Top view of FESEM images of TiO_2 nanotubes anodized at 5 minutes.

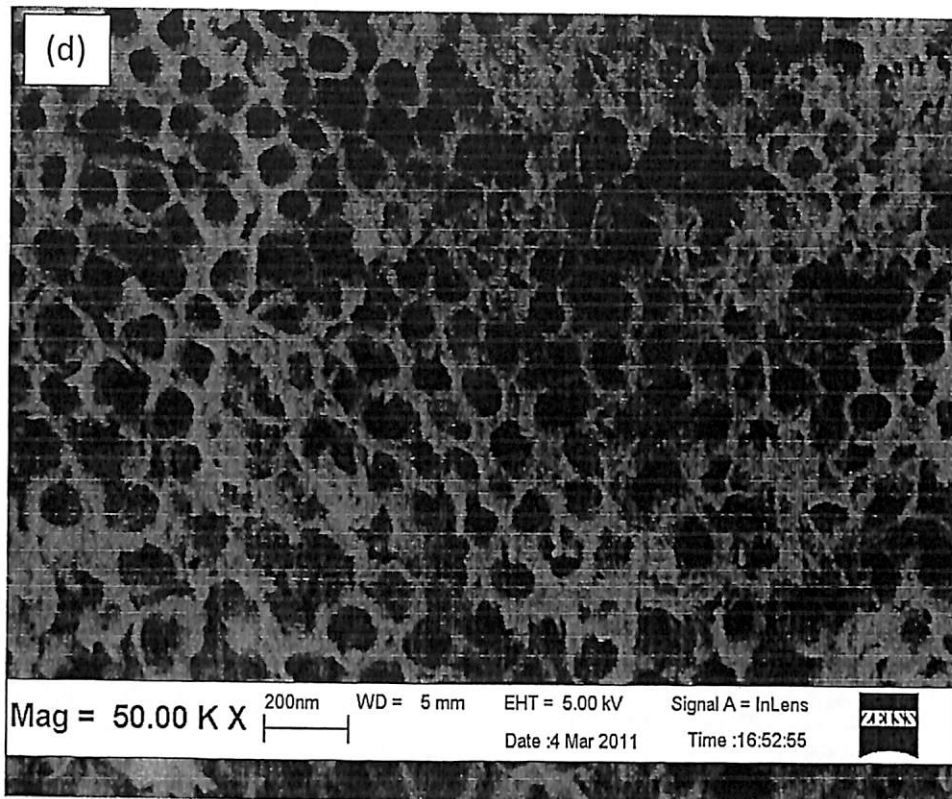


Figure 10d: Top view of FESEM images of TiO₂ nanotubes anodized at 10 minutes.

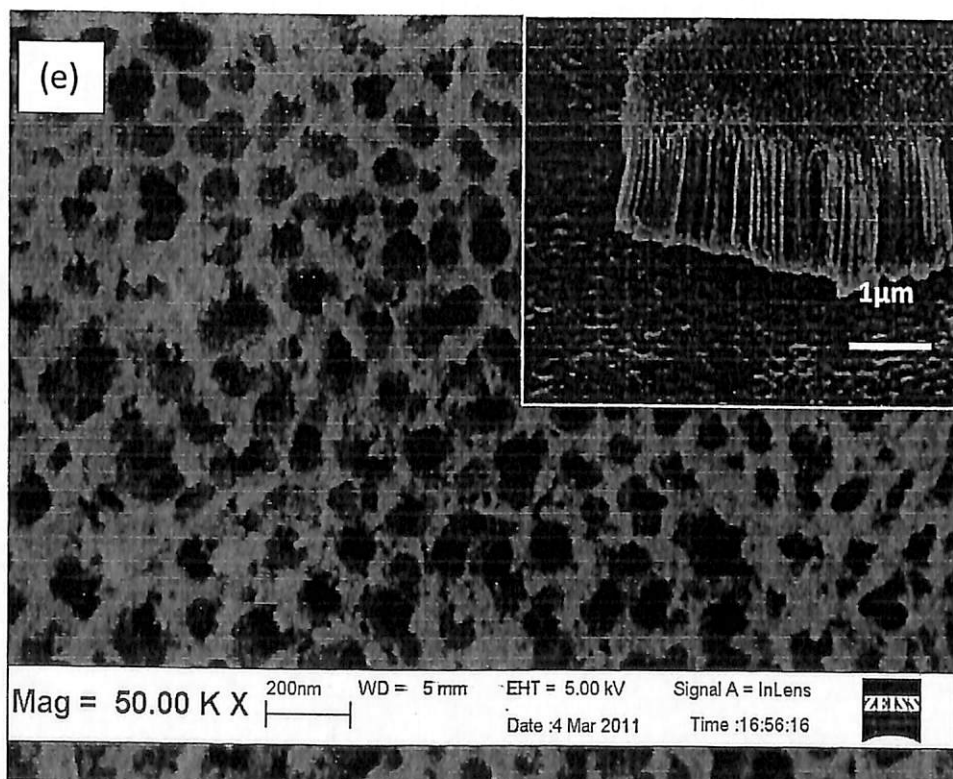


Figure 10e: Top view of FESEM images of TiO₂ nanotubes anodized at 15 minutes, The inset shows cross sectional view.

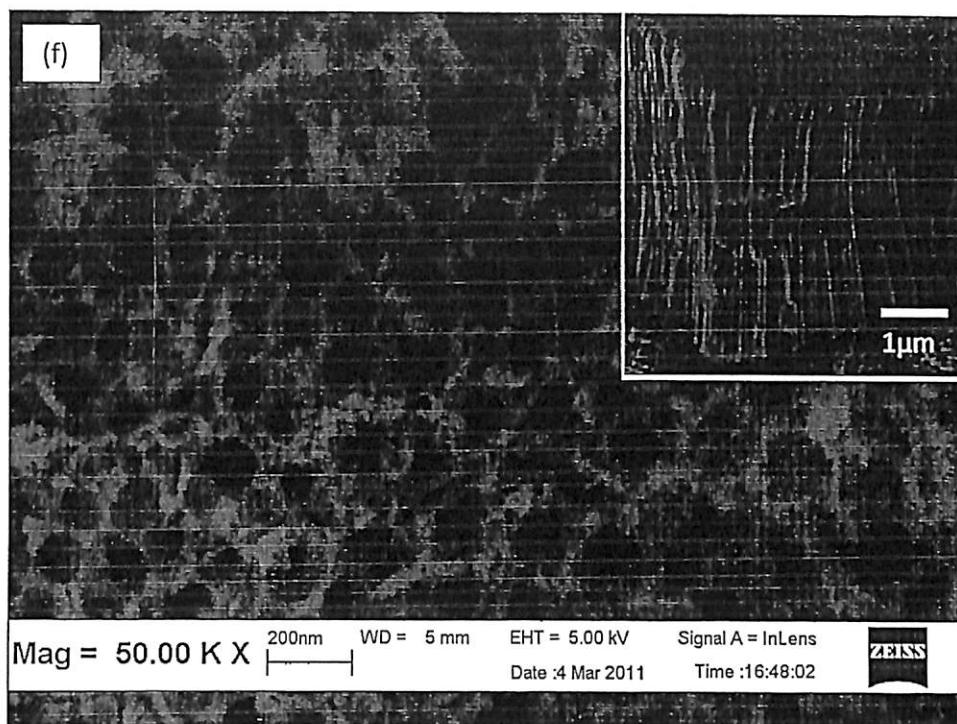


Figure 10f: Top view of FESEM images of TiO_2 nanotubes anodized at 30 minutes. The inset shows cross sectional view.

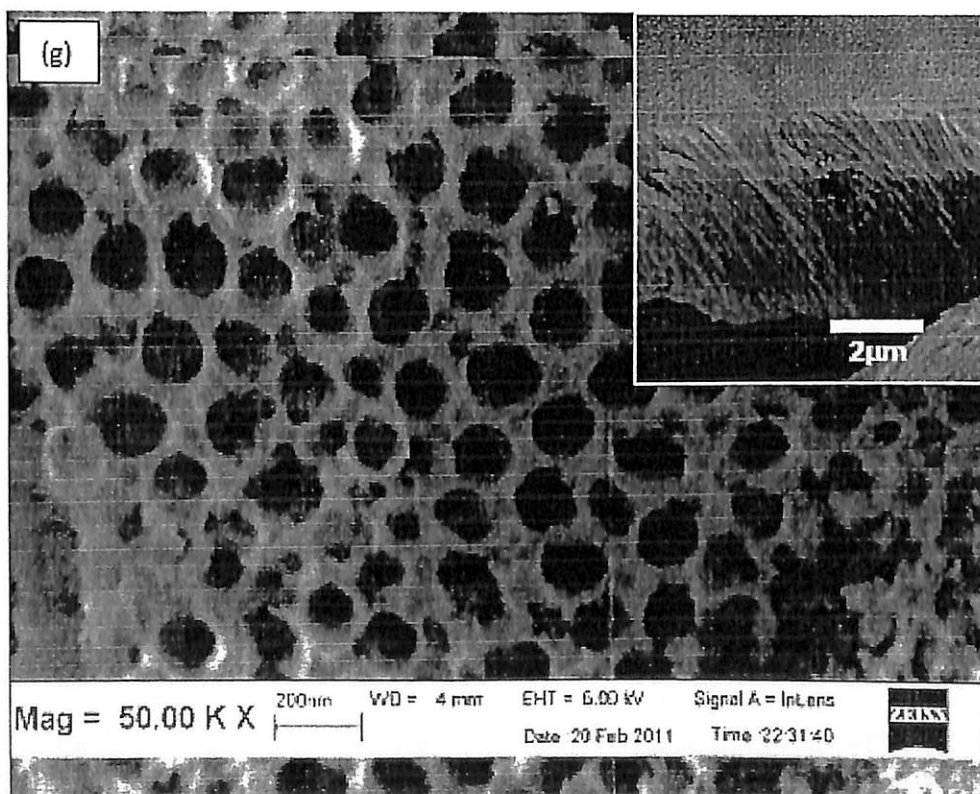


Figure 10g: Top view of FESEM images of TiO_2 nanotubes anodized at 6 hours. The inset shows cross sectional view of the respective samples.

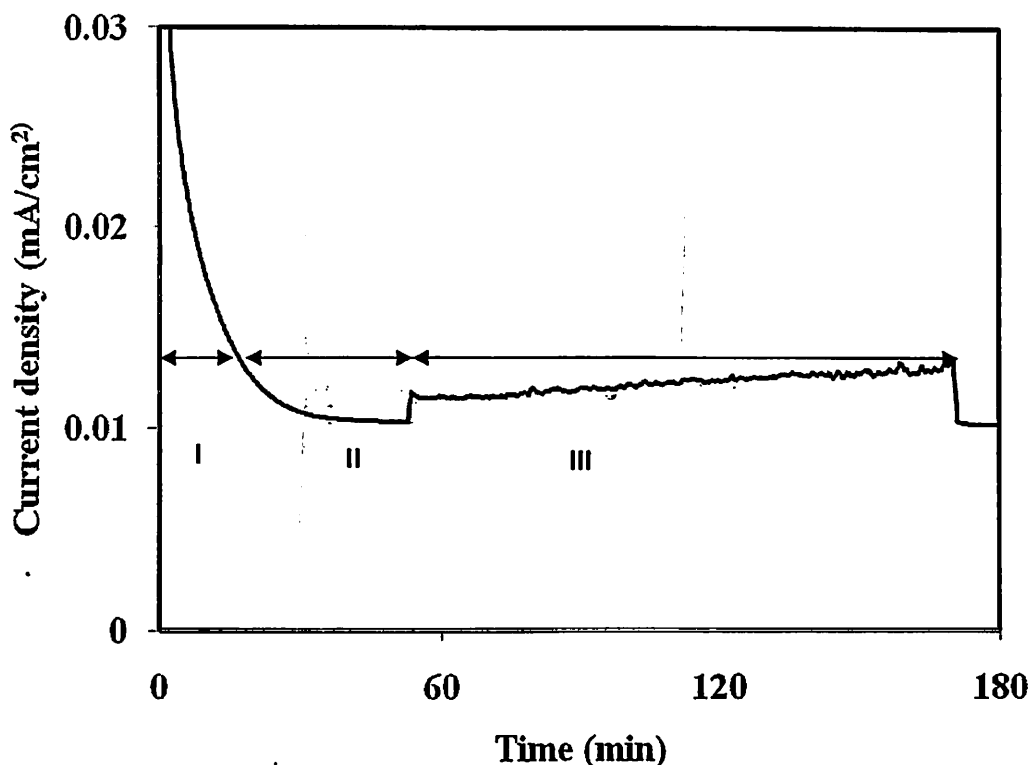


Figure 11: Current density profile of Ti alloy

Figure 11 shows the current density profile recorded during anodization. Three stage of current density were observed in ethylene glycol. Stage 1, represent formation of oxide layer, stage 2 signified nucleation of nanoporous and stage 3 denoted formations of nanotubes. Growth of nanotubes structure occurred at stage 3 where by the length of the nanotubes increased from 2.8 to 6.4 μm .

Effect of annealing temperature

Figure 12 shows the XRD pattern of the as anodized and annealed TiO_2 nanotubes at different temperatures. The result clearly shows the crystal structure of TiO_2 depends on the annealing treatment. The XRD of the as-anodized sample indicate amorphous structure as only α and β -Ti peaks were observed. Annealing at 400°C has promoted the crystallization of anatase phase at 2θ of 25° and 48°, corresponding to (101) and (200) plane, respectively. Dominant structure of the sample annealed at 600 °C is rutile, implies complete transformation from anatase to rutile at this temperature.

The morphology of the as anodized TiO_2 without heat treatment and annealed at 500°C, 550°C as well as 600°C are shown in Figure 13. a,b,c and d, respectively. The sample heat treated at 400°C is discussed previously in section 4.1. Overall, the results show the robustness of TiO_2 nanotubes formed on Ti alloy is temperature dependent. The nanotubes structure is sustained till 400°C. At 500°C and 550°C, thickening of titania nanotubes wall occurred due to mass transport involving Ti^{4+} diffusion at the bottom and wall of the TiO_2 nanotubes. Finally, at 600°C, tubular structure is completely damaged and nanorod like structure is formed. The schematic diagram explaining the morphologies changes with temperature are illustrated in Figure 14.

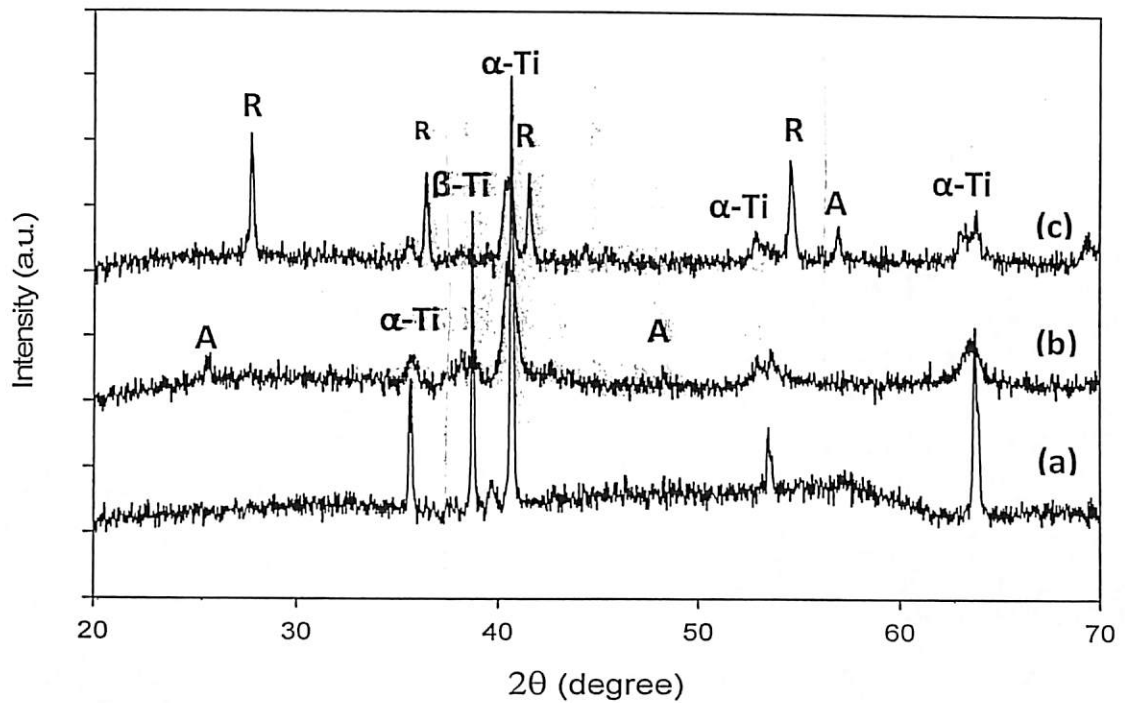


Figure 12: XRD pattern of the annealed Ti-6Al-4V alloy sheets with different crystalline structure, (a) amorphous sample, (b) 400°C, (c) 600 °C. α -Ti = Alpha -Ti, β -Ti = Beta- Ti, A = Anatase, R = Rutile

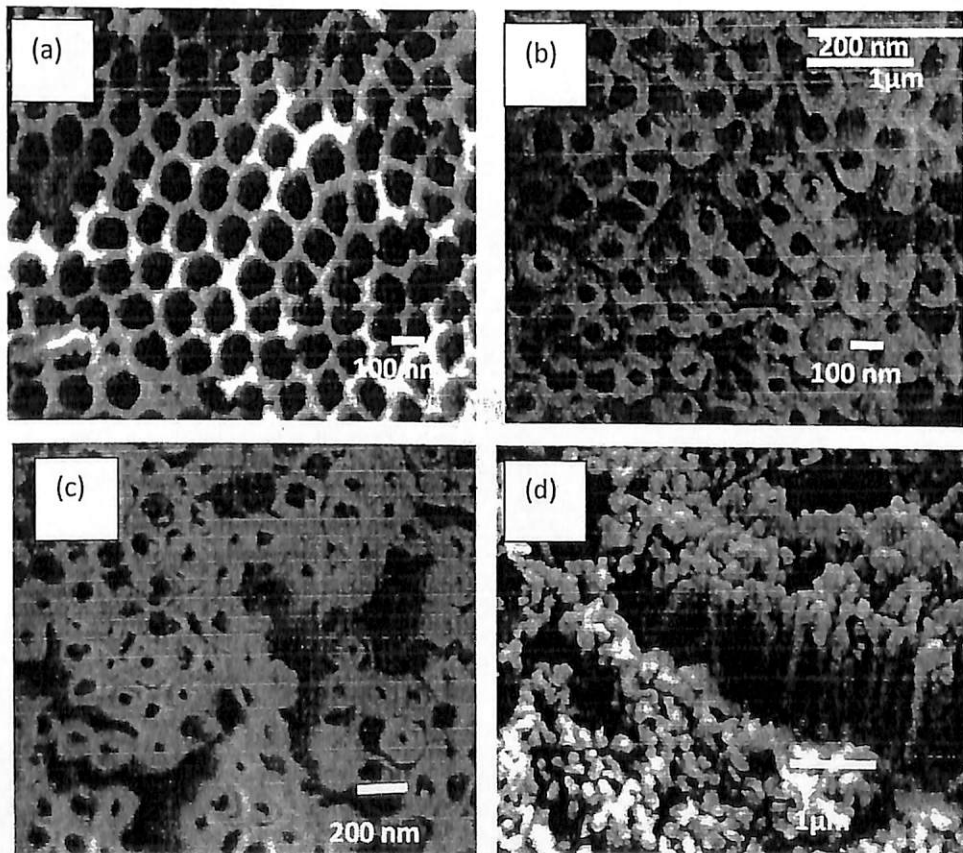


Figure 13: FESEM images of as anodized TiO_2 nanotubes without heat treatment (a), and annealed at 500 °C (b), 550 °C (c) and 600 °C (d).

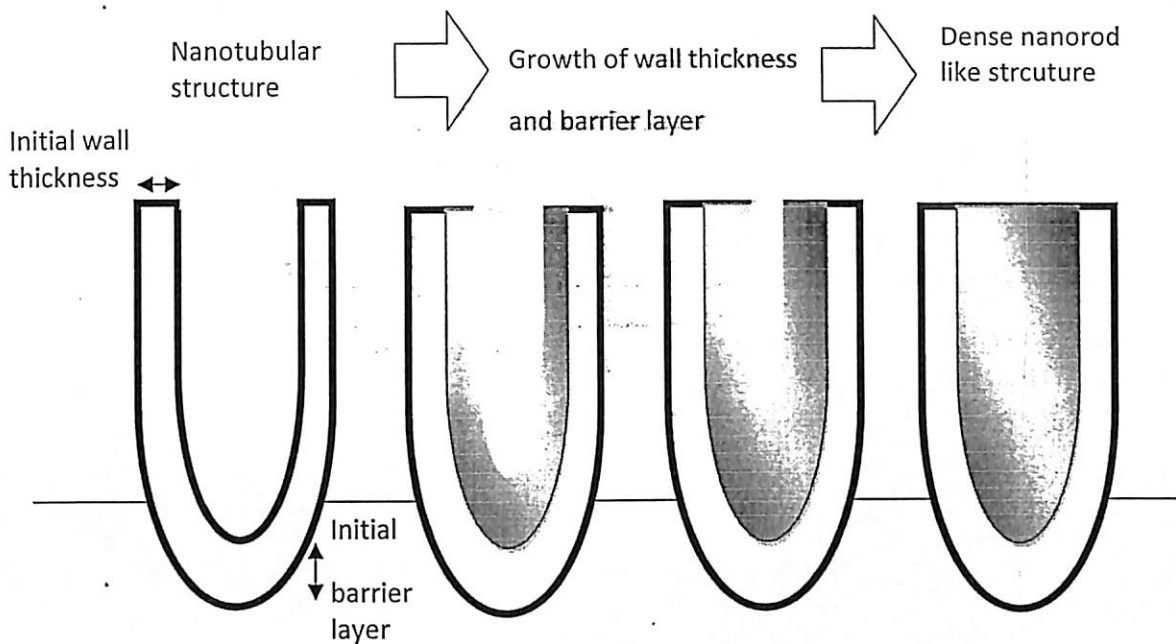


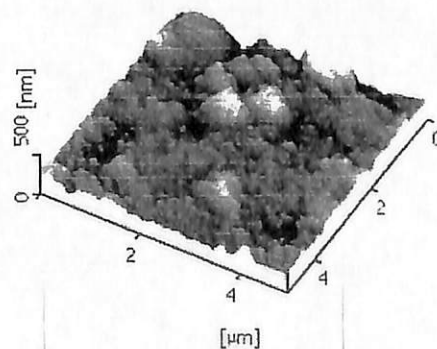
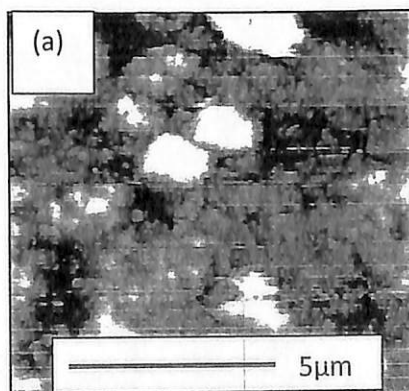
Figure 14: Schematic illustration to show the growth of the nanotubes during thermal annealing

Surface Roughness

AFM topographic maps of as anodized and annealed TiO_2 are shown in Figure 15 a-c. The surface roughness parameter R_a , R_q and Z range of each sample were examined and summarized in Table 3. It can be seen that higher annealing temperature induces higher roughness level as a consequence of an increased in densification of the nanotubes.

Table 3: The roughness parameter obtained upon annealing temperature variation

Annealing temperature ($^{\circ}\text{C}$)	0	400	600
Roughness Parameters (nm)			
R_a (average)	48.65	67.25	95.97
RMS	60.49	84.56	122.60
Z range (max.-min.)	292.30	521.10	646.90



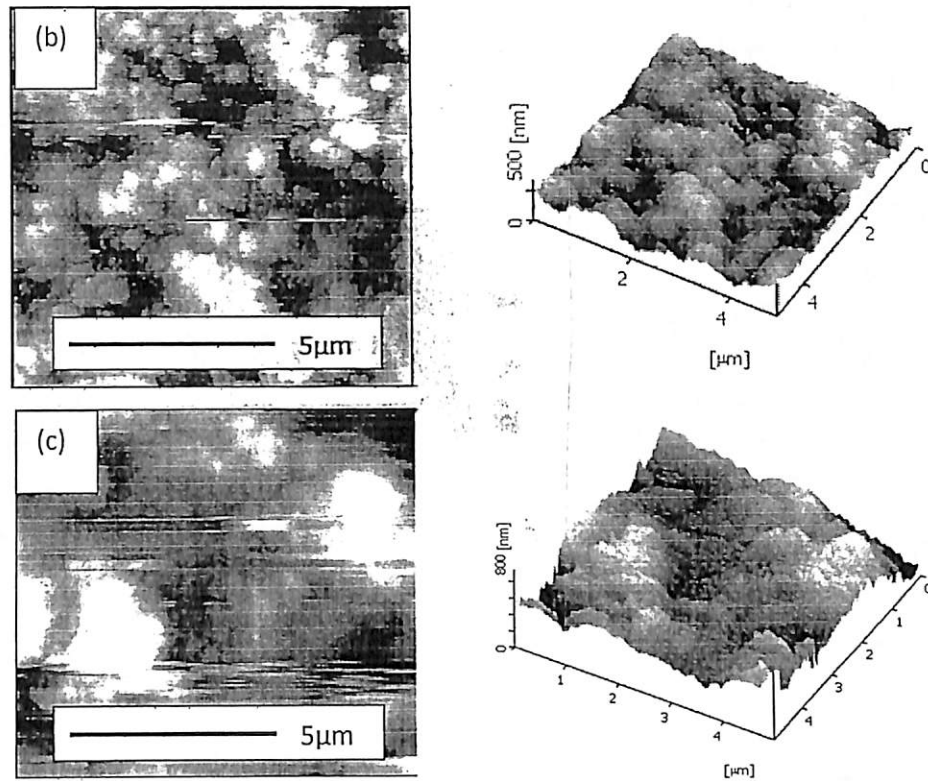


Figure 15: AFM topography and 3D morphology of TiO₂ nanotube (a) 0°C (b) 400°C and (c) 600°C

Cell interaction

In this part, the behavior of cellular interaction on three different types of anatase, amorphous and rutile TiO₂ using fibroblast cells line was done. MTS assay was performed to study the cells viability. The cellular activities of cell viability for fibroblast cells on three different types of crystal structures are shown in Figure 16. Cell proliferation is the attachment of the cells on the material surface. The results shows no significant value obtained for 24 and 48 hours of cell culture for all three crystal structures. At 72 hours, amorphous structure has significant value; this reveals increase in proliferation HS27 cells on as-anodized TiO₂ nanotubes surface. This show HS27 fibroblast cells has better cellular interaction on amorphous TiO₂ nanotubes as compared to anatase or rutile. It also indicates that fibroblast cells like surface with lower surface roughness of about 49 to 60 nm.

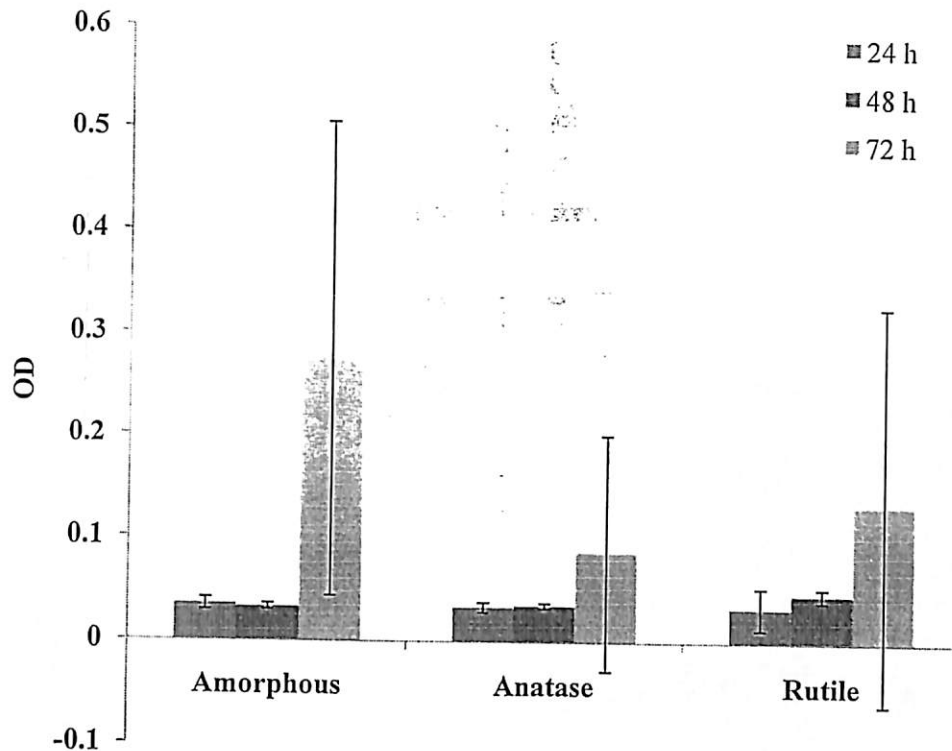


Figure 16: MTS assay data showing the optical density (OD) of reaction product of the MTS working solution with HS27 fibroblast cells cultured as-anodized, annealed at 400°C and 600 °C amorphous TiO₂ nanotubes, and heat-treated (anatase) TiO₂ nanotubes after 24 h, 48 h, and 72 h of incubation. The error bars in the figure represent the standard deviation for four samples for each data.

Conclusion

The TiO₂ nanotubes were fabricated on Ti-6Al-4V alloy by anodization process. Optimized condition for formation of TiO₂ on Ti alloy are: electrolyte with 99 ml ethylene glycol + 1 ml H₂O + 0.7 g NH₄F, voltage 60 V and time of anodization is 60 minutes. TiO₂ nanotubes with average diameter of 110 nm and 3.1 μm length are obtained. Cell interaction study on Ti alloy with various crystalline structure on fibroblast cells line showed that amorphous structure possess good proliferation, followed by anatase and rutile phase.

References

- Das, Bose, Bandyopadhyay, (2009) Enhanced Fatigue Performance of Porous Coated Ti6Al4V Biomedical Alloy, 225.
- Li, Xiao, Liu. (2008) Synthesis And Bioactivity Of Highly Ordered TiO₂ Nanotube Arrays Applied Surface Science, 255. 365–367
- Luo, Yang, Liu, Fu, Sun, Yuan, Zhang, Liu. (2008). Fabrication And Characterization Of Self-Organized Mixed Oxide Nanotube Arrays By Electrochemical Anodization Of Ti-6Al-4V Alloy Materials Letter, s 62.4512–4515
- Matykinaa, & J. M. (2011). Morphologies Of Nanostructured Tio₂ Doped With F On Ti-6Al-4V Alloy, Electrochimica Acta, 56, 2221–2229.
- Shankar, Mor, Prakasam, Yoriya, Paulose, Varghese, Grimes. (2007) Highly-ordered TiO₂ nanotube arrays up to 220 μm in length: use in water photoelectrolysis and dye-sensitized solar cells Nanotechnology 18, 1-11

Sreekantan, Saharudin, Lockman, & Tzu. (2010). Fast-Rate Formation Of TiO₂ Nanotube Arrays In An Organic Bath And Their Applications In Photocatalysis. *Nanotechnology*, 21


Yu, Jiang, Zhang & Xu, L. (2010). The Effect Of Anatase TiO₂ Nanotube Layers On MC3T3-E1 Preosteoblast Adhesion, Proliferation, And Differentiation. 1012-1021.



FUNDAMENTAL RESEARCH GRANT SCHEME
FINAL REPORT ASSESSMENT FORM
Borang Penilaian Laporan Akhir
Skim Geran Penyelidikan Fundamental

A.	TITLE OF RESEARCH: <i>Tajuk penyelidikan:</i>	<i>Formation of Nanotubular TiO₂ Bioactive Oxide Layer on Titanium and Cell Response Studies</i>				
B.	PERSONAL PARTICULARS OF RESEARCHER / Maklumat Penyelidik:					
(i)	Name of Research Leader: <i>Nama Ketua Penyelidik:</i>	<i>Dr. Sreemala Sreekantan</i>				
(ii)	School/Institute/Centre/Unit: <i>Pusat Pengajian /Institut/Pusat/Unit:</i>	<i>Pusat Pengajian Kejuruteraan Bahan & Sumber Mineral</i>				
(iii)	Phone No. (Office): <i>No. Tel. (Pejabat):</i>					
(iv)	Hand Phone No: <i>No. Telefon Bimbit:</i>					
(v)	Fax. No: <i>No. Faks:</i>					
C.	SUMMARY OF ASSESSMENT <i>(Tick (✓) the appropriate box. Also, provide additional comments in Section F)</i>	Inadequate		Acceptable	Very Good	
		1	2	3	4	5
1.	Achievement of Project Objectives	<input type="checkbox"/>	<input type="checkbox"/>	<input checked="" type="checkbox"/>	<input type="checkbox"/>	<input type="checkbox"/>
2.	Quality of Output	<input type="checkbox"/>	<input type="checkbox"/>	<input checked="" type="checkbox"/>	<input type="checkbox"/>	<input type="checkbox"/>
3.	Quality of Organisational outcomes	<input type="checkbox"/>	<input type="checkbox"/>	<input checked="" type="checkbox"/>	<input type="checkbox"/>	<input type="checkbox"/>
4.	Quality of sectoral/national impacts	<input type="checkbox"/>	<input type="checkbox"/>	<input checked="" type="checkbox"/>	<input type="checkbox"/>	<input type="checkbox"/>
5.	Technology Transfer / Commercialization Potential	<input type="checkbox"/>	<input type="checkbox"/>	<input type="checkbox"/>	<input type="checkbox"/>	<input type="checkbox"/>
6.	Quality and Intensity of Collaboration	<input type="checkbox"/>	<input type="checkbox"/>	<input checked="" type="checkbox"/>	<input type="checkbox"/>	<input type="checkbox"/>
7.	Overall Financial Expenditure	<input type="checkbox"/>	<input type="checkbox"/>	<input checked="" type="checkbox"/>	<input type="checkbox"/>	<input type="checkbox"/>
8.	Overall Assessment of Benefits	<input type="checkbox"/>	<input type="checkbox"/>	<input checked="" type="checkbox"/>	<input type="checkbox"/>	<input type="checkbox"/>

D	OUTPUT SUMMARY				
1	Achievement Percentage				
	Project progress according to milestones achieved up to this period	25%	50%	75%	100%
					✓
2	Research Findings				
		ISI Journal	International Journal	National Journal	
	Number of articles/ manuscripts/ books	1			
		International		National	
	Paper presentations				
	Others (Please specify)				
3	Human Capital Development				
		Number			
		On-going		Graduated	
		M'sian	Non- M'sian	M'sian	Non- M'sian
	Ph D Student				
	M Sc Student				
	Undergraduate Final Year Project			2	
	Temporary Research Officer				
	Temporary Research Assistant				
	Others (Please specify)				
	Total				

E.	ACTION TO BE TAKEN (Tick (✓) the appropriate boxes)	
	<input checked="" type="checkbox"/>	Project file to be closed. (For financial and administration purposes)
	<input type="checkbox"/>	Project to be Reviewed Once Additional Information Has Been Obtained by the Project Leader (Please see section E)
	<input type="checkbox"/>	Forward to Innovation Office for Consideration: <input type="checkbox"/> Patent <input type="checkbox"/> Commercialisation <input type="checkbox"/> Technology Transfer <input type="checkbox"/> Others (Please specify): _____
	<input type="checkbox"/>	Forward to Division of Industry & Community Network (DICN)
	<input type="checkbox"/>	Others (Please specify): _____ (E.g.: Formations of teams or cluster etc.)
F.	Additional information to be provided by the Project Leader [Please provide details of the specific information being requested from the project Leader in the areas identified in Section E]	
G.	Comments Regarding Assessment [Please provide below an explanation of any assessment made in Section C showing a rating below "acceptable"]	
H.	Overall Comments: <i>Average output .</i> Name of Panel: <u><i>Prof Bassim H Hamid</i></u> Signature : <u></u> Date : <u><i>9/4/2012</i></u>	
I.	Endorsement & Comments/Suggestions of Research Dean: Signature: _____ Date : _____	